

# Faculdade de Engenharia da Universidade do Porto



**FEUP**

## **Regeneration of the peripheral nerve - Development and evaluation of guide tubes of biodegradable polymer**

Joana Maria da Silva Gomes

Dissertation  
Integrated Master in Bioengineering

Supervisor: José Domingos da Silva Santos (PhD)  
Co-Supervisor: Ana Colette Pereira de Castro Osório Maurício (PhD)

June 2014

© Joana Gomes, 2014



# Resumo

Danos nas fibras nervosas periféricas resultam em perda axonal e desmielinização, seguidos de regeneração e remielinização sob condições ideais com a possibilidade de alguma recuperação funcional. Estudos recentes indicam que a diferença na regeneração axonal entre o sistema nervoso periférico (PNS) e o sistema nervoso central (CNS) resulta da presença de fatores permissivos presentes no PNS e fatores inibitórios ativos presentes no CNS.

Pacientes com lesões no nervo periférico estão muitas vezes no auge da sua atividade laboral, o que faz da regeneração do nervo periférico um foco principal de pesquisa. Assim, o desafio experimental consiste em acelerar a regeneração axonal para promover a reinervação e melhorar a recuperação funcional após uma lesão no nervo periférico. Algumas das abordagens experimentais para melhorar a recuperação funcional incluem a aplicação focal de fatores neurotróficos, o bloqueio de moléculas inibidoras da regeneração axonal e o transplante de células.

Depois de ocorrer uma lesão quer de axonotmese quer de neurotmese, os axónios periféricos têm a capacidade de se regenerar e de se ligar novamente aos seus alvos, sendo que no primeiro caso não há necessidade de reconstrução cirúrgica uma vez que o endoneuro, perineuro e epineuro são mantidos. No entanto, o estado funcional resultante pode não ser o melhor uma vez que a regeneração é demorada e conduz à atrofia neurogénica dos músculos regionais. Na prática clínica, a reparação cirúrgica ideal em situações de neurotmese (seccionamento total do nervo) considera-se ser a sutura topo-a-topo, de modo a aproximar o topo distal do topo proximal, sem haver tensão no local da sutura. Alternativamente, nervos autólogos são o *gold standard* deste tipo de procedimentos sempre que ocorre perda de substância e não seja possível executar uma sutura topo-a-topo sem tensão. No entanto, o uso de autoenxertos está limitado pelos inconvenientes inerentes uma vez que requer uma segunda cirurgia, com sacrifício de um nervo funcional, o que resulta em perda sensorial e morbidade do local de doação, entre outros.

Nas últimas décadas, os diferentes tipos de enxertos artificiais ou biológicos foram desenvolvidos e investigados para que pudesse ser estabelecida uma relação entre eles e os enxertos de nervos autólogos em termos dos resultados da regeneração do nervo e da

recuperação funcional. Estes tubos-guia são projetados para preencher a lacuna existente num nervo seccionado quando existe um *gap*, para limitar a fibrose e orientar as fibras em regeneração na direção do topo distal. O enxerto de nervo artificial é um canal tubular feito de materiais sintéticos ou biodegradáveis e que pode orientar a regeneração do axónio sem inibir o crescimento e maturação. O canal tubular pode ser implantado vazio ou preenchido com fatores de crescimento, células ou fibras. Devido à sua capacidade de renovação, multiplicação e diferenciação, as células estaminais mesenquimatosas (MSCs) têm sido usadas para suplementar os tubos-guia, sendo que foi já demonstrado que estas se podem diferenciar em células neuronais e células da glia.

Em termos de *design*, os tubos-guia são semelhantes e podem ser feitos de diferentes biomateriais, sejam eles naturais, tais como o alginato ou o quitosano, ou sintéticos, tal como o ácido poliglicólico (PGA), utilizando diferentes métodos de fabricação.

O quitosano é amplamente utilizado para aplicações biomédicas, devido à sua biocompatibilidade e atividade antibacteriana e também pode ser associado com outros produtos de acordo com a necessidade da aplicação. Neste trabalho, foram produzidos tubos-guia de quitosano sendo que se procedeu à sua implantação no modelo animal do nervo ciático de ratos adultos. Foram feitas teses funcionais assim como uma caracterização mecânica e estrutural dos tubos-guia.

# Abstract

Damage to peripheral nerve fibers results in axonal loss and demyelination followed by regeneration and remyelination under optimal conditions with the possibility of some functional recovery. Recent studies indicate that the difference between peripheral nervous system (PNS) and central nervous system (CNS) axonal regeneration is the result of both permissive factors present in the PNS and active inhibitory factors present in the CNS.

Patients with peripheral nerve injury are often at the peak of their employment productivity which makes peripheral nerve regeneration a prime focus of research. Hence, the experimental challenge is to accelerate axonal regeneration to promote reinnervation and improve functional recovery after peripheral nerve injury. Some of the experimental approaches to enhance functional recovery include focal application of neurotrophic factors, blockade of axonal regeneration inhibitory molecules and cell transplantation.

After an injury, whether it is one of axonotmesis or one of neurotmesis, peripheral axons have the ability to regenerate themselves and to reconnect with their targets. In the first case, there is no need to perform a surgical reconstruction because the endoneurium, perineurium and epineurium structure is maintained. However, the functional outcome may not be the best since the regeneration process takes a long time and it leads to neurogenic atrophy of the regional muscles. In clinical practice, the ideal surgical repair in neurotmesis cases (complete sectioning of the nerve) is considered to be the end-to-end coaptation, by closing the distance between the proximal and the distal stumps, without associated tension in the suture. Alternatively, autologous nerves are the gold standard in this type of procedures every time there is loss of matter and if it is not possible to perform an end-to-end suture without tension. However, autograft nerve grafting is limited by the inherent drawbacks since it requires a second surgery, with sacrifice of a functional nerve, which results in donor sensory loss and pain and donor site morbidity, among others.

In the past few decades, different types of biological or artificial grafts have been developed and investigated so a comparison could be established between them and the autologous nerve grafts in terms of the outcomes of nerve regeneration and functional

recovery. These guide tubes are designed to bridge the gap of a sectioned nerve, to limit the fibrosis process and to orient the regenerating fibers towards the distal stump. The artificial nerve graft is a tubular conduit of synthetic or biodegradable materials, which could guide axon regeneration without inhibiting growth and maturation. The conduit may be implanted empty or it may be filled with growth factors, cells or fibers. Due to their ability to renovate, multiply and differentiate, mesenchymal stem cells (MSCs) have been used to supplement guide tubes being that it has already been demonstrated that they can differentiate into neuronal and glial cells.

In terms of design, the guide tubes are similar but they can be made of different biomaterials, whether they are natural, such as alginate or chitosan, or synthetic, such as polyglycolic acid (PGA), using various fabrication methods.

Chitosan is widely used for biomedical applications because of its biocompatibility and antibacterial activity and it can also be assembled with many other products, depending on the need of the application. In this work, chitosan guide tubes were produced and implanted using the rat sciatic nerve animal model. Functional tests were performed as well as a mechanical and structural characterization of the guide tubes.

# Acknowledgment

I would like to thank my supervisor Professor José Domingos Santos and my co-supervisor Professor Ana Colette Maurício for giving me the opportunity to be part of their work group, for the guidance and help whenever needed.

I would like to thank Dina Silva for being such a good listener, for all the advices and for helping me every time I needed.

I would also like to thank Carla Ferreira, Vitor Sencadas, Daniela Correia and Renato Gonçalves for being tireless, interested, supportive and always so nice to me.

Finally, I would like to thank my dearest friends from Guimarães, Porto and Braga and to the most important people in my life, my parents.





# Table of contents

Resumo .....	iv
Abstract.....	vi
Acknowledgment.....	viii
Table of contents .....	x
List of figures.....	xii
List of tables.....	xiv
Abbreviations.....	xvi
<b>Chapter 1.....</b>	<b>1</b>
Introduction.....	1
<b>Chapter 2.....</b>	<b>3</b>
Literature review .....	3
2.1. The Peripheral Nervous System .....	3
2.1.1. Schwann Cells .....	4
2.1.2. Node of Ranvier .....	5
2.1.3. Sodium Channels .....	5
2.2. Nerve Injury .....	6
2.2.1. Wallerian Degeneration.....	7
2.2.2. Axonal Sprouting .....	7
2.3. Traditional Treatments .....	7
2.3.1. Autologous Nerve Grafts.....	8
2.3.2. Allografts.....	9
2.4. Tissue Engineered Nerve Grafts.....	9
2.4.1. Requirements of an Ideal Scaffold.....	11
2.4.1.1. Biocompatibility .....	11
2.4.1.2. Biodegradability .....	12
2.4.1.3. Permeability.....	12
2.4.1.4. Biomechanical Properties .....	13
2.4.1.5. Surface Properties .....	13
2.4.2. Natural Biomaterials in Neural Scaffolds .....	13
2.4.2.1. Acellular Allogeneic or Xenogeneic Tissues.....	13
2.4.2.2. Naturally-derived Biopolymers.....	14
2.4.2.2.1. Alginate .....	14
2.4.2.2.2. Chitosan.....	15

2.4.2.3. Synthetic Materials .....	16
2.5. Nerve Scaffold Functionalization .....	16
2.5.1. Neurotrophic Factors .....	17
2.5.2. Support Cells.....	17
2.5.2.1. Mesenchymal Stem Cells .....	18
2.6. Additional approaches .....	19
<b>Chapter 3.....</b>	<b>20</b>
Preliminary Experimental Work .....	20
3.1 Culture of Mesenchymal Stem Cells .....	20
3.2 Animal Model .....	21
3.3 Experimental Procedure .....	22
3.4 Samples analysis .....	22
3.5 Histological study .....	24
3.6 Final considerations .....	25
<b>Chapter 4.....</b>	<b>26</b>
Experimental Work .....	26
4.1 Materials and Methods .....	26
4.1.1. Preparation of the guide tubes.....	26
4.1.2. Structural characterization of the guide tubes.....	27
4.1.2.1. Scanning Electron Microscopy (SEM) .....	27
4.1.2.2. Fourier Transform Infrared (FTIR) Spectroscopy.....	27
4.1.2.3. Water uptake assay .....	27
4.1.2.4. Determination of the degree of crosslinking .....	28
4.1.2.5. Mechanical assay .....	28
4.1.3. <i>In vivo</i> Testing .....	29
4.1.3.1. Ethics and Regulation.....	29
4.1.3.2. Microsurgical Procedure .....	29
4.1.3.3. Functional Assessment.....	31
4.1.3.3.1. Evaluation of Motor Performance and Nociceptive Function .....	31
4.1.3.3.2. Sciatic functional index and static sciatic index.....	31
4.1.3.3.4. Sciatic nerve stereology and histological analysis.....	32
4.1.4 Statistical analysis .....	33
4.2 Results .....	33
4.2.1 SEM.....	33
4.2.2 FTIR .....	34
4.2.3 Water uptake .....	34
4.2.4 Degree of crosslinking.....	35
4.2.5 Mechanical assay .....	36
4.2.6 <i>In vivo</i> Testing .....	37
4.2.6.1 EPT and WRL .....	37
4.2.6.2 SFI and SSI .....	38
4.2.6.3 Stereological and histological analysis .....	39
4.3 Discussion .....	40
4.4 Conclusions.....	42
4.5 Future Work.....	43
<b>References .....</b>	<b>46</b>
<b>Appendix .....</b>	<b>53</b>

# List of figures

Figure 1 - Peripheral motor neuron showing the cell body, axon extension surrounded by a myelin sheath and the axons terminals (left). A cross section of the neuron shows the myelin sheath, composed of Schwann cells (right). <sup>12</sup> .....	4
Figure 2 - Schematic representation of the degenerative and regenerative events associated with peripheral nerve injury. <sup>2</sup> .....	6
Figure 3 - NGC model showing the progression of events during peripheral nerve regeneration. <sup>12</sup> .....	11
Figure 4 - MSCs from Wharton's jelly exhibiting a mesenchymal-like shape with a flat polygonal morphology (left). After 72h of culture in neurogenic medium the cells became exceedingly long and there is a formation of typical neuroglial-like cells with multibranches (right) (x100). .....	21
Figure 5 - Hydrogel after 3 days. ....	23
Figure 6 - MSCs and hydrogel after 3 days. ....	23
Figure 7 - Hydrogel after 15 days. ....	24
Figure 8 - Chitosan-GPTMS (left) and PLGA (right) guide tubes before implantation. ....	27
Figure 9 - Chitosan-GPTMS membrane assembled in the universal testing machine. ....	29
Figure 10 - Rat sciatic nerve before (A) and after neurotmesis (B), followed by the nerve reconstruction with a chitosan-GPTMS guide tube (C and D). ....	30
Figure 11 - SEM images of the chitosan-GPTMS guide tubes. ....	33
Figure 12 - FTIR spectrum of chitosan-GPTMS guide tubes (A) and chitosan powder (B). ....	34
Figure 13 - Averaged values of water uptake (%) of the chitosan-GPTMS guide tubes as function of the period of soaking in PBS. ....	35
Figure 14 - Calibration curve of glycine. ....	35
Figure 15 - Optical absorbance of the chitosan powder and the chitosan-GPTMS guide tubes. ....	36
Figure 16 - Strain-stress curves of both hydrated and dry samples. ....	36

Figure 17 - Mean Extensor Postural Thrust (EPT) and Withdrawal Reflex Latency (EPT) results for 20 weeks follow-up. Values of Motor Deficit were obtained performing EPT test (A). Values in seconds (s) were obtained performing WRL test to evaluate the nociceptive function (B). These tests have been performed pre-operatively (week 0), at week 1 and every 2 weeks after the surgical procedure until week 20, when the animals were sacrificed for morphological analysis. .... 38

Figure 18 - Rat footprints taken during the SSI test. On the left are represented the footprints taken on week 1 and week 2. On the right are represented the footprints taken on week 4. .... 39

Figure 19 - Histological appearance of a normal rat sciatic nerve (Magnification: 1000x). .... 40

# List of tables

Table 1 - Histological scoring ..... 24

Table 2 - Values of strain (%), stress (MPa) and Young modulus (E) (MPa) for both hydrated and dry samples. .... 37

Table 3 - Results of the Extensor Postural Thrust (EPT). .... 53

Table 4 - Results of the Withdrawal Reflex Latency (WRL). .... 54

Table 5 - Stereological quantitative assessment of density, total number, diameter and myelin thickness of regenerated sciatic nerve fibers at week 20 after neurotmesis. Values are presented as mean  $\pm$  SD. .... 54



# Abbreviations

BDNF - brain-derived neurotrophic factor  
CNS - central nervous system  
DPSCs - dental pulp stem cells  
ECM - extracellular matrix  
EPT - extensor postural thrust  
ESCs - embryonic stem cells  
FCT - Fundação para a Ciência e Tecnologia  
FDA - Food and Drug Administration  
GPTMS -  $\gamma$ -glycidoxypropyltrimethoxysilane  
MSCs - mesenchymal stem cells  
NGCs - nerve guidance conduits  
NGF - nerve growth factor  
NHN - ninhydrin  
PBS - phosphate buffered saline  
PCL - poly-caprolactone  
PGA - polyglycolic acid  
PLA - polylactic acid  
PLCL - poly-DL-lactide-co-caprolactone  
PLG - glycolic acid  
PLGA - poly(L-lactic-co-glycolic acid)  
PLLA - poly(L-lactic acid)  
PNS - peripheral nervous system  
SFI - sciatic functional  
SSI - sciatic static index  
VGSCs - voltage-gated sodium channels  
WRL - withdrawal reflex latency







# Chapter 1

## Introduction

It is estimated that about 2.8% of trauma patients, many of whom acquire life-long disability, are affected by peripheral nerve injuries. In Europe, over 300,000 cases of peripheral nerve injury occur annually and in the United States approximately 360,000 people suffer from upper extremity paralytic syndromes annually.<sup>1,2,3</sup>

Peripheral nerve lesions are caused primarily by traffic accidents, tumour resection or side effects resulting from surgeries like orthopaedic and cosmetic facial interventions.<sup>4</sup> Unlike what happens in the central nervous system (CNS) of mammals, the peripheral nervous system (PNS) has a permissive environment provided by the Schwann cells, whereas the CNS has active inhibitory factors that elicit growth cone collapse.<sup>5</sup> Recent works have shown that the PNS has an intrinsic regenerative ability to a certain extent.<sup>1</sup>

The regeneration of peripheral nerves has been a field of study for many years and an accelerated development has been seen in finding new and better strategies to repair peripheral nerves. However, the clinical application of state-of-the-art approaches is still limited, being that the most relevant functional outcomes are not completely satisfactory and depend on many factors including the size and location of injured nerves as well as the age of patients.<sup>1</sup>

Peripheral nerve injuries may include or not gaps between the nerve stumps. If when an injury occurs an intervention is not made, functional regeneration becomes restricted due to scars, neuroma formation, mismatched fibers or extensive splitting of the re-growing axons.<sup>6</sup> Axonotmesis involves severance or destruction of peripheral nerves without any damage to connective tissue such as the endoneurial tubes, which remain intact. The interruption of axons is the result of nerve pinching, crushing or prolonged pressure.<sup>2</sup> In neurotmesis the nerve is completely transected, being that nerve loss may or not occur. Without a surgical reconstruction the axonal regrowth is impossible, making this the most challenging type of peripheral nerve injury repair.<sup>6,2</sup>

The main challenges, when facing surgical management of the injury, is the survival of the damaged neurons, the establishment of a microenvironment that eases the neurite outgrowth and the guidance of axons to their target for appropriate reinnervation.<sup>1</sup> Furthermore, microsurgical methods of treatment have been shown to be very effective despite the residual disability that often persists for the lifetime of the patient.<sup>4</sup> Thus, there is a clear need to understand the fundamental events that occur during an injury and the cellular and molecular requirements for a successful nerve regeneration process.<sup>2,7</sup>

The tissue engineering approach is to repair, complement and regenerate damaged tissue by using materials that will support and reinforce the regenerating tissue. One of the strategies is to build three-dimensional, porous scaffolds which role is to manipulate cell functions since they provide spaces and surface area enough for cell adhesion and proliferation, and to supply oxygen and nourishment. Besides these characteristics, scaffolds should be biocompatible and biodegradable, have a large surface to volume ratio, and be mechanically strong and capable of being formed into desired shapes and structures.<sup>8</sup>

In the case of peripheral nerve injury, tissue engineering often associates biomaterials, such as chitosan and PCL, to cellular systems, which should be helpful to improve nerve regeneration, in terms of motor and sensory recovery, and also by shortening the healing period avoiding regional muscular atrophy.<sup>7</sup>

Even in PNS, nerve regeneration is still a very complex phenomenon that is far from being fully understood. However, with the advancement of tissue engineering and regenerative medicine it is expected that nerve grafts with a close similarity to native nerve tissue will be eventually developed and clinically applied.<sup>1</sup>

The state-of-the-art presented in Chapter 2 was carried out in order to gather information about peripheral nerve regeneration, including the different strategies and approaches being studied and implemented when it comes to regenerate neurons that somehow have been injured.

# Chapter 2

## Literature review

A literature review is presented in this section. Initially, the anatomy of the PNS will be addressed, followed by the explanation of the series of events that occurs after an injury. Most importantly, it will be addressed the requirements of a nerve graft, the strategies already implemented in the clinic and the approaches to be implemented in the future.

### 2.1. The Peripheral Nervous System

Neuroglial cells are quite different from nerve cells since they do not directly participate in the synaptic interactions and electrical signalling.<sup>9</sup> These cells in both the PNS and the CNS have been regarded simply as the 'glue' that holds physically and metabolically the nervous system together. They are major players alongside the neurons of the PNS and the CNS.<sup>10</sup> Additionally, they provide a scaffold for some aspects of neural development and aid in recovery from neural injury.<sup>9</sup>

All neurons in the PNS are in intimate physical contact with Schwann and satellite cells, regardless of whether they are myelinated or not, sensory or autonomic. All axons of the peripheral nerves are sheathed by rows of Schwann cells (Figure 1), in the form of either one Schwann cell to each axonal length or in Remak bundles, formed when an individual Schwann cell envelopes lengths of multiple unmyelinated axons.<sup>10,11</sup>

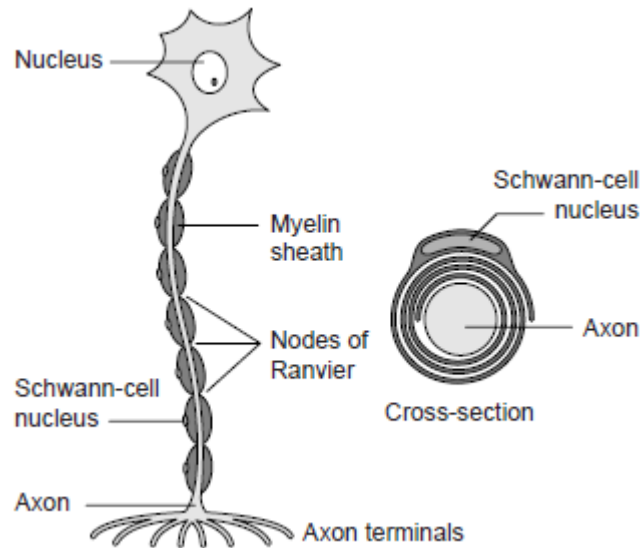


**Figure 1** - Peripheral motor neuron showing the cell body, axon extension surrounded by a myelin sheath and the axons terminals (left). A cross section of the neuron shows the myelin sheath, composed of Schwann cells (right).<sup>12</sup>

### 2.1.1. Schwann Cells

Like the oligodendrocytes, Schwann cells are responsible for the production of the specialised, unique and complex spirals of myelin membrane. They can be categorized by their morphology, antigenic phenotype, biochemistry and anatomical location.<sup>9,10,11</sup>

Myelin-forming Schwann cells have a profound impact in both the healthy and diseased nervous system, not only on axonal conduction but also on many properties of the axons themselves. Non-myelin-forming Schwann cells are in close contact with unmyelinated fibers, which are small-diameter axons of C fibers originating from sensory ganglia and axons from sympathetic neurons. These cells envelop a number of axonal lengths to form Remak bundles. It is becoming apparent that they are vital for the function and maintenance of unmyelinated axons and also necessary for pain sensation.<sup>5,10</sup>

Satellite cells have a distinct partnership with the neuronal cell they ensheath and are directly associated with the cell body rather than the axon of a neuron, so that each neuronal cell body in the dorsal root ganglia is surrounded by a cap of several satellite Schwann cells.<sup>6</sup> Some studies suggest that they have specific roles given their location and unique interaction with the sensory neuronal cell bodies they envelope.<sup>10</sup>

Another feature of peripheral nerves is the presence of a continuous basal lamina tube that surrounds individual myelinated fibers and groups of nonmyelinated fibers for the entire length of the nerve. Also, there is the deposition of extracellular collagen in the endoneurial compartment.<sup>5</sup>

The columns of Schwann cells, called bands of Büngner, are an indispensable pathway for directed axonal regeneration and provide an important permissive environment for axonal regeneration. Axons regenerate within these basal lamina tubes to reach motor or sensory

targets. If regenerating axons do not grow within this environment, but through the endoneurial space within the connective tissue, they stop regenerating and do not reach their target.<sup>5</sup>

The interdependence between Schwann cells and neurons underpins the functioning of the entire PNS. There is also a symbiotic relationship between them, since each one is dependent on the other for normal development, function and survival.<sup>13</sup> On one hand, the axon controls the initiation of myelination, the number of myelin lamellae and the maintenance of the complex Schwann cell organization. On the other hand, Schwann cells regulate axonal diameter, neurofilaments spacing and phosphorylation, and the clustering of ion channels at the node of Ranvier in myelinated axons.<sup>10</sup>

The PNS regenerative powers are in part due to intrinsic properties of Schwann cells that encourage spontaneous regeneration. PNS axonal regeneration occurs through the initiation of signalling cascades that activate Schwann cells to produce neurotrophic factors, cytokines, extracellular matrix (ECM) and adhesion molecules, which aid in regrowth of the injured nerve.<sup>14,15</sup> This is in contrast to CNS neuroglia, in which astrocytes produce an hostile environment for axonal regeneration in response to injury.<sup>10</sup>

Interactions between the PNS and other systems during development and maintenance should be considered. This becomes particularly important when it comes to the endocrine and immune systems which can have a considerable impact on the function of the PNS. Schwann cells play a crucial role in maintaining the equilibrium between the PNS and the immune system, being that their potential immunocompetence suggests that they can induce an immune response within the peripheral nerve.<sup>16</sup>

### **2.1.2. Node of Ranvier**

The node of Ranvier is a segment as long as a millimetre of axon between adjacent Schwann cells and it is the site of action potential generation. The action potential of myelinated axons is generated at the relatively narrow node of Ranvier and skips from node to node, providing saltatory conduction.<sup>5</sup>

### **2.1.3. Sodium Channels**

Sodium channels are the molecular batteries responsible for generating action potentials and they are present at the node of Ranvier in relatively high concentrations.<sup>5</sup>

There are numerous sodium channel subtypes with different electrical properties. It has been established that the sodium channel subtype Nav 1.6 is the tetrodotoxin-sensitive, kinetically fast channel present at the normal node of Ranvier of peripheral nerve fibers.<sup>5</sup>

Voltage-gated sodium channels (VGSCs) are members of the ion channel protein family and play an essential role in neuronal and non-neuronal function, being responsible for the

initiation and propagation of action potentials in excitable cells by allowing the influx of sodium ions.<sup>17</sup> The very high density of VGSCs at the Ranvier node is important because synchronous activation of these channels provides substantial current to ensure the efficacy of activation of the next set of nodes and high-fidelity saltatory conduction. Moreover, for fast conducting regenerated myelinated axons to be functional, they must recapitulate appropriate nodal and myelin architecture.<sup>5</sup>

The newly formed nodes of Ranvier of the regenerated axons expressed sodium channel subtype Nav 1.6, the normal predominant nodal sodium channel. This indicates that engraftment of exogenous Schwann cells into injured nerve can reconstitute myelin and appropriate sodium channel organization necessary for proper impulse conduction.<sup>5</sup> In the sodium channel subtype Nav 1.6, tetrodotoxin binds to neurotoxin receptor within the outer vestibule of the VGSC and blocks the influx of sodium ions by occluding the outer pore of the channel. This binding inhibits the propagation of action potentials, thereby paralyzing nerve and muscle function.<sup>17</sup>

## 2.2. Nerve Injury

When peripheral nerve fibers are damaged the result is often axonal loss and demyelination followed by regeneration over short distances and remyelination under optimal conditions with the possibility of at least some functional recovery.<sup>1,5</sup> The anatomy of axons goes through some changes after an injury and is characterized by primary degeneration with the distal portion of the severed cable being left non-functional, followed by a regenerative response of the proximal stump (Figure 2). However, in order to have an optimal recovery of nerve function, the outgrowing axons of the proximal portion of the nerve need to migrate their way through the distal one. This way, these axons will be guided back to their proper target innervation site.<sup>18</sup>

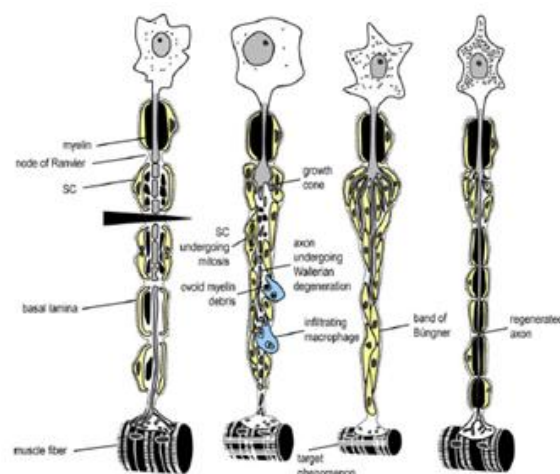


**Figure 2** - Schematic representation of the degenerative and regenerative events associated with peripheral nerve injury.<sup>2</sup>



### **2.2.1. Wallerian Degeneration**

When peripheral nerves are transected, a series of molecular and cellular events are triggered throughout the distal stump of the transected nerves and within a small zone distal to the proximal stump. This is called the Wallerian degeneration and it results in the disintegration of axoplasmic microtubules and neurofilaments.<sup>1</sup> Then, the axon diebacks a millimetre or two from the injury site and the distal segment degenerates. Within one day, most axons of the distal stump of transected nerves are reduced to granular and amorphous debris, which are then phagocytized by macrophages and monocytes. While the axon segment distal to the injury site degenerates, the Schwann cells proliferate typically within the basal lamina and form a longitudinal column of Schwann cells (band of Büngner).<sup>1,5</sup>

### **2.2.2. Axonal Sprouting**

Roughly two days after the nerve injury, the proximal stump of the nerve gives rise to axonal sprouts that will extend either on the surface of Schwann cells or to the inner laminin-rich surface of the basal lamina of the bands of Büngner. New axonal sprouts usually emanate from the nodes of Ranvier. In cases where both the proximal and distal nerve segments appose each other, regenerating axons may grow through these Schwann cell “scaffolds” and make contact with peripheral targets with the possibility of some functional recovery.<sup>1,5</sup>

Under the influence of neurotrophic factors and ECM molecules produced by Schwann cells, several axonal sprouts are issued from a single regenerating fiber and grow within a single band of Büngner. After making contact with the target, all but one of the sprouts dieback leaving a single fiber making contact with a peripheral target. The regenerated fiber is then myelinated by Schwann cells and signal conduction velocity is increased to appropriate levels. Usually, regenerated and remyelinated axons have shorter internodes, thinner myelin, and smaller axonal diameters, but nevertheless they can achieve rapid conduction.<sup>5</sup> In humans, axon regeneration occurs at a rate of approximately 2-5 millimetres a day which means that significant injuries may take many months to heal.<sup>1</sup>

However, sometimes the regenerating axon sprouts do not reach and elongate enough through the trophic distal Schwann cell tube. When this happens, they grow in a more random manner and form a neuroma, which is often the case after limb amputation. These sprouts present changes in the mechanosensitivity and chemosensitivity, which is associated to paresthesia and phantom limb.<sup>5</sup>

## **2.3. Traditional Treatments**

Peripheral nerve regeneration is a process which depends on many factors, such as the large quantity and high speed of axonal outgrowth, the remyelination of axons by Schwann cells, and the maturity of regenerating nerve fibers. In several studies, the incorporation of support cells and/or growth factors has proven effective for modulating the above cellular

behaviours. This has been evidenced by a wide range of animal experiments, but it has not yet come to clinical use due to multiple barriers.<sup>1</sup>

Several clinical interventions have been attempted for many years now in order to aid the repair of peripheral nerve injuries. During the 19<sup>th</sup> and 20<sup>th</sup> centuries a wide range of surgical techniques has been put into use for the management of peripheral nerve injuries.<sup>1</sup>

The surgical techniques used to repair these kinds of injuries are classified into two general categories: manipulative nerve operations and bridge operations. The first includes direct neurorrhaphy, which is the surgical suturing of a divided nerve, and nerve transfers or neurotization and it is usually performed in the situation of no nerve tissue loss and possible approximation with minimal tension. Neurorrhaphy is only applicable to short nerve gaps because the fascicular coaptation may cause excessive tension over the suture line, which would inhibit nerve regeneration. Neurotization involves taking nerves or even nerve branches with redundant functions and transferring them to the target site in order to restore function of the severed nerves.<sup>1</sup>

In cases where nerve loss is substantial, physicians often chose to interposition a nerve graft between the proximal and distal nerve stumps. The typical choice is to use an autologous nerve graft which is a functional but less important nerve segment self donated such as sural nerves, superficial cutaneous nerves or lateral and medial forearm nerves.<sup>19</sup>

### **2.3.1. Autologous Nerve Grafts**

Autologous nerve grafting remains the gold standard technique, with an 80% recovery rate, to which other alternative treatments are compared. However, there are many drawbacks and disadvantages associated with this technique, such as limited availability of donor nerves, the need for a second surgery to obtain the donor nerve, donor site morbidity and secondary deformities, as well as mismatch between the injured nerve and the donor nerve.<sup>1</sup>

Nerve grafts must fulfil some requirements when being placed in the injury site. The graft must not only cover the defect between the proximal and distal nerve stumps, it must also provide the optimal conditions and environment for axonal regeneration, such as Schwann cells, revascularization and endoneurial morphology.<sup>4</sup> In addition, one of the major problems in surgical treatment is ends coaptation in the case of large loss of nerve tissue. Also, finding substitute implants that are not rejected by the organism is a requirement for the success of the technique.<sup>4</sup>

Target reinnervation is one of the cellular events that predetermine functional recovery after peripheral nerve repair. When a nerve is transected with a damage of basal lamina tubes, axonal sprouts are not restrained to their original basal lamina tubes and axons become unable to grow faithfully along original pathways to their target regions. The mismatch of regenerated axons to their targets may contribute, at least in part, to unsatisfactory functional recovery after nerve grafting.<sup>1</sup>

### 2.3.2. Allografts

An alternative technique to autologous grafts is allografts. These are decellularized grafts that constitute an effective technique clinically adopted for peripheral nerve regeneration applications. Decellularized nerve allografts carry the benefit of preserving the basal lamina/ECM of the nerve, potentially leading to mechanical guidance of regenerating axons. They may also provide another potential technology to bridge critically sized defects.<sup>20</sup>

AxoGen's Avance<sup>®</sup> is an example of a decellularized allograft that has been used in the clinic to repair facial nerve and hand nerve defects.<sup>20,21</sup> This allograft uses a protocol involving detergents and chondroitinases in the process of decellularization.<sup>18</sup> However, in a study comparing different acellular allografts in a rat sciatic nerve defect it was found a superior performance in detergent-treated allografts than in AxoGen-treated and cold-preserved allografts.<sup>22</sup> When it comes to functionalization, none of these approved conduits have incorporated adhesive ECM proteins or neurotrophic factors.<sup>18</sup>

This generation of conduits provides mainly physical guidance via conduit morphology in order to help to direct the damaged nerve to its target. The next generation will seek to increase nervous system function by using topographical and protein cues that interact with nervous tissue at the cellular level. These cues should also be tailored to the nerve and function of interest.<sup>18</sup>

By developing biocompatible and anisotropic nerve guidance conduits (NGCs), tissue engineering offers clinical potential for peripheral nerve repair. The upcoming generation should be able to incorporate the use of neurotrophic factors, ECM proteins, surface micropatterning and favorable physical and mechanical properties.<sup>18</sup>

## 2.4. Tissue Engineered Nerve Grafts

In the last few decades, different types of biological or artificial grafts have been developed and investigated having as comparison autologous nerve grafts in terms of the outcomes of nerve regeneration and functional recovery.<sup>1</sup> Also, the tissue engineering field has grown in the sense of offering great opportunities to investigators and surgeons to develop tissue engineered nerve grafts. These are usually composed of a physical scaffold with support cells and/or growth factors or other biomolecular components.<sup>1</sup>

Tissue engineered nerve grafts, or neural scaffolds, have many purposes. They direct axons sprouting from the proximal to the distal nerve stump, they maintain adequate mechanical support for the regenerating nerve fibers, and provide a conduit channel for the diffusion of neurotrophic factors secreted by the damaged nerve stump and a conduit wall for the exchange of nutrients and waste products (Figure 3). Also, these neural scaffolds prevent the infiltration of fibrous scar tissue that hinders axonal regeneration and create an optimal microenvironment for nerve regeneration through the accumulation and release of exogenous and endogenous biochemical effects.<sup>1</sup>

The first generation of artificial nerve conduits clinically used was nonresorbable silicone tubes which covered the gap between the proximal and the distal stumps of a transected peripheral nerve. Clinical trials involved the resection of a rat sciatic nerve portion which was then encased by a cylindrical silicone chamber. However, these chambers were plagued by compression and often required secondary surgeries for removal.<sup>18,23</sup> Ever since, a variety of different materials was approved for clinical use.

Currently, there are some FDA-approved bioresorbable conduits being commercialized such as NeuroTube<sup>®</sup> (PGA), Neurolac<sup>®</sup> (PLCL) and NeuraGen<sup>®</sup> (type I collagen).<sup>18</sup>

Despite their approval and success, some of these products present some issues which ultimately lead to their loss of efficacy. For example, Neurolac<sup>®</sup> initially showed promising results with regard to sensory recovery but later on it showed problems of biocompatibility, swelling, degradation rate and automutilation.<sup>24</sup> NeuraGen<sup>®</sup> has also reported excellent clinical success for the surgical repair of brachial plexus birth injuries. However, it has been shown in a rat sciatic nerve model that processed nerve allografts behave significantly better than NeuraGen<sup>®</sup> in critically sized defects.<sup>25</sup> Neurotube<sup>®</sup> represents a positive trend for short gaps. For digital nerve defects less than or equal to 3 centimeters, the conduit offered a higher percentage of patients with “excellent recovery,” though data was not statistically significant.<sup>18,26</sup> Nevertheless, for critically sized defects in humans, which are characterized for being greater than 3 centimeters in length, NGCs are yet to approach the effectiveness of the gold standard, nerve autografts.<sup>18</sup>

One of the purposes of Tissue Engineering nowadays is to associate NGCs made of biomaterials to other biological components that may have a decisive role in the final result of the peripheral nerve regeneration. The ultimate goal of this association is to improve nerve regeneration when it comes to motor and sensory recovery and to shorten the healing process avoiding regional muscular atrophy.<sup>27</sup>

Using NGCs alone have been shown to be effective in terms of peripheral nerve regeneration but only until a certain point. When nerve gaps are over 30 millimeters, neural scaffolds only allow the bridging between the stumps. However, in order to have an effective regeneration, supporting cells and growth factors should be incorporated in the NGC.<sup>28</sup> The cellular systems may include Schwann cells, mesenchymal stem cells and marrow stromal cells which may produce growth factors or ECM molecules or modulate the inflammatory process.<sup>28</sup> These growth factors are important components of NGCs because they may enhance regeneration by promoting axonal outgrowth and neuronal survival.<sup>29</sup> Besides cellular systems and growth factors, hydrogels may also be included in the NGCs architecture. They can be used as a physical barrier to protect the cells from hostile extrinsic factors or as a matrix to cell adhesion, growth and differentiation to further improve the secretion of therapeutic proteins by the cells.<sup>30</sup>

When considering the use of these neural scaffolds in the clinic there are some requirements that they have to fulfil such as being easy to fabricate and sterilize, simple to implant in the body by microsurgical techniques, biocompatible and biodegradable.

Biomechanical and surface properties are also major concerns. These requirements are mainly determined by the scaffold material and structure.<sup>1</sup>

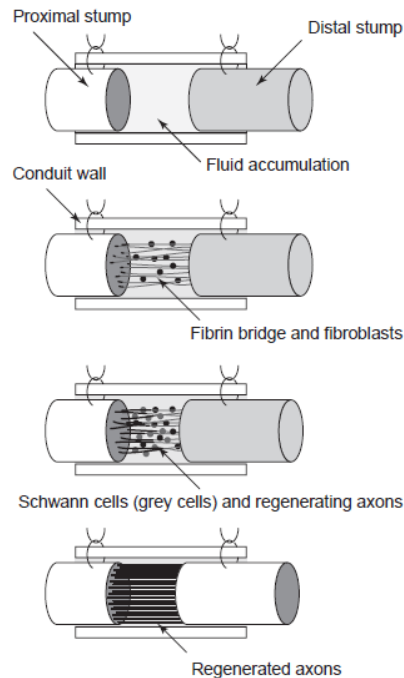


Figure 3 - NGC model showing the progression of events during peripheral nerve regeneration.<sup>12</sup>

## 2.4.1. Requirements of an Ideal Scaffold

### 2.4.1.1. Biocompatibility

According to the original definition, biocompatibility is the ability to serve as a substrate that supports the appropriate cellular behaviours. These include the promotion of molecular and mechanical signalling systems to aid nerve regeneration, without eliciting any undesirable effects on neural cells and tissues and/or inducing undesirable local or systemic responses in the eventual host.<sup>31</sup>

When in contact with blood, neural scaffolds must not induce hemolysis, destroy blood components or lead to coagulation and thrombus formation. The scaffold must also not have toxic effect on the surrounding tissues, neither teratogenicity nor gene mutation. On the other hand, these tissues should not induce corrosive effects or immune rejection on the scaffold. Finally, mechanical compatibility focuses on the matching of mechanical properties between the scaffold and the nerve tissue.<sup>1</sup>

In order to analyse the biocompatibility of a new developed biomaterial for nerve regeneration, it is important to analyse the inflammatory response of the surrounding tissues before its application in nerve defects. For that purpose the evaluation should be a standard

and effective one. The International Organization for Standardization is a worldwide federation of international standard-setting bodies. ISO 10993-6:2007 was developed to specify test methods for the assessment of the local effects after implantation of biomaterials intended for use in medical devices.<sup>32</sup> This section of ISO 10993 applies to materials that are solid and non-biodegradable, degradable and/or resorbable and non-solid such as porous materials, liquids, pastes and particulates. This part of ISO 10993 does not deal with systemic toxicity, carcinogenicity, teratogenicity or mutagenicity.<sup>33</sup> The test specimen is implanted into a site and animal species appropriate for the evaluation of the biological safety of the material. These implantation tests are not intended to evaluate or determine the performance of the test specimen in terms of mechanical or functional loading. The local effects are evaluated by a comparison of the tissue response caused by a test specimen to that caused by control materials used in medical devices of which the clinical acceptability and biocompatibility characteristics have been established.<sup>32</sup> The goal of these test methods is to characterize the history and evolution of the tissue response after implantation of a medical device/biomaterial including final integration or resorption/degradation of the material. Investigators must follow these guidelines when performing tests in animal models.<sup>27,30</sup>

#### **2.4.1.2. Biodegradability**

Ideally, a nerve scaffold should possess a controllable ability to degrade *in vivo*.<sup>1</sup> Therefore, non-degradable materials may not be advisable since they may become detrimental by virtue of toxicity or tendency to constrict nerve remodelling.<sup>1</sup> Also, the degradation rate should be tuned to match the regeneration rate of the nerve.<sup>1</sup>

#### **2.4.1.3. Permeability**

Neural scaffolds construction must take into consideration the necessary gas and nutrient exchange and also the fluids exchange between the regeneration environment and surrounding tissues through pores in the conduit wall. The permeability of the scaffolds influences the formation of the fibrin matrix during the initial period of regeneration which leads to the conclusion that an increased permeability allows the mass transport and capillary in-growth, while maintaining a barrier to fibroblasts. Also, the permeability of NGCs may be needed for the viability of supportive cells.<sup>19,29</sup>

There are different techniques through which NGCs can be made permeable, including by cutting holes into the wall, rolling of meshes, fibre spinning, adding salt or sugar crystals and injection-molding evaporation.<sup>29</sup>

#### **2.4.1.4. Biomechanical Properties**

Some biomechanical properties must be considered when designing neural scaffolds. One of them is the Young modulus, also known as elastic modulus, that should be similar to the one of the nerve tissues in order to resist *in vivo* physiological loads.<sup>1</sup>

Some of the natural polymers used to make NGCs have a low mechanical strength. In order to fulfil the mechanical requirements, these polymers may be chemically modified and crosslinked with other structural components such as synthetic polymers.<sup>3</sup>

During the nerve regeneration process, nerve scaffolds should have the capacity to withstand mechanical stress from neighbour tissues and maintain some elasticity and bendability without collapse or losing shape. They should also mechanically support the axonal sprouting between the injured nerve sprouts.<sup>19</sup> Thus, a balance should be found between the hardness and the flexibility of the scaffold because scaffolds too stiff are easy to cause dislocation and scaffolds too flexible fail to support axonal regeneration.<sup>1</sup>

#### **2.4.1.5. Surface Properties**

The functionalization of the surface of neural scaffolds can influence the interactions between these structures and the nerve cells. Longitudinally oriented texture can be added to the surface, which has been shown to influence directional outgrowth of axons and uniform alignment of Schwann cells *in vitro*, resulting in better outcomes in nerve regeneration *in vivo*.<sup>34</sup>

In addition, nanofibrous scaffolds have attracted research interest because they offer unique surface chemical properties such as high surface area favourable for cell attachment and growth and topographical signals favourable for directing cellular functions.<sup>35</sup>

### **2.4.2. Natural Biomaterials in Neural Scaffolds**

#### **2.4.2.1. Acellular Allogeneic or Xenogeneic Tissues**

As an alternative to autologous nerve grafts, other autologous non-nerve tissues, like muscles, veins, tendons and epineurial sheaths have been tested as structures to bridge peripheral nerve gaps. However, this approach showed limited success and still suffers from the problem of inadequate availability due to the autologous origin.<sup>36</sup>

In contrast, allogeneic or xenogeneic tissues, which are either nerve tissues or non-nerve tissues, can be harvested from living donors, fresh corpses or animals, rather than from the patient, and thus they are used as the material for neural scaffolds with a potentially unlimited supply. Furthermore, amnion harvested from human placental tissues can be also employed as an allogeneic or xenogeneic tissue-derived material for preparing neural scaffolds.<sup>1</sup>

However, the nerve grafts made up of allogeneic or xenogeneic tissues are inevitably limited by immune responses of the host when they are implanted *in vivo*.<sup>37</sup> At the time of

the implantation, immunosuppressive drugs must be administered to patients, which may leave them susceptible to infections and tumour formation.<sup>38</sup>

When it comes to decellularization methods, freezing-thawing, sonication, and agitation are the common physical treatments, while chemical treatments are mainly performed by using various detergents.<sup>1</sup> Since decellularization focuses on removal or destruction of the immunogenic cells and preservation of the ECM components that are essentially conserved between species, the resulting cell-free tissues can be used to prepare nerve grafts as a very appropriate alternative to autologous nerve grafts, especially in the repair of non-critical peripheral nerve gaps with a small length and diameter.<sup>39</sup>

#### **2.4.2.2. Naturally-derived Biopolymers**

Collagen, laminin and fibronectin are some of the insoluble components of the ECM that play an important role in the development and growth of axons.<sup>40</sup> Other proteoglycans and glycosaminoglycans of the ECM can modulate neural activity and neuritis extension, providing either stimulatory or inhibitory effects.<sup>41</sup> Thus, ECM components have become important candidate materials for neural scaffolds, being processed into lumen fillers of NGCs in the form of fibers, channels, porous sponges or hydrogels to serve as delivery vehicles for support cells, growth factors or drugs.<sup>1</sup>

As previously mentioned, there are at the moment some FDA-approved, commercially available conduits which purpose is to regenerate peripheral nerves. One of these conduits is NeuraGen<sup>®</sup> which main constituent is type I collagen. However, gelatin derived from denatured collagen has also been investigated for a wide range of biomedical applications.<sup>42</sup> Gelatin was the first biodegradable material examined for preparing neural scaffolds, and gelatin-based neural scaffolds can be covalently incorporated with additional bioactive cues, which are gradually released during the scaffold biodegradation.<sup>43</sup>

##### **2.4.2.2.1. Alginate**

Commonly purified from seaweed, alginate is a naturally occurring copolymer of  $\beta$ -D-mannuronate and  $\alpha$ -L-guluronate and a biodegradable polysaccharide.<sup>4</sup> This biopolymer has been implanted in sciatic nerve gaps in both rats and cats in the form of foam and the results showed that it could promote peripheral nerve regeneration.<sup>44</sup>

In another study using cats which underwent severing of the right sciatic nerve, the gap was treated with both tubulation and non-tubulation repair. It was used a PGA mesh tube filled with alginate sponge. Successful axonal elongation and reinnervation in both the afferent and efferent systems were detected. Intracellular electrical activity was also recorded, which is directly indicative of continuity of the regenerated nerve and restoration of the spinal reflex circuit.<sup>45</sup>

Several other studies were performed in order to evaluate the response of the nervous system after nerve severing and implantation of an alginate conduit. One of these studies suggested that by simply filling the nerve gap using an alginate sheet the nerve can be



regenerated and erectile function may be restored.<sup>46</sup> In another study, it was concluded that alginate gel presents a good biocompatibility for regenerating axon outgrowth and Schwann cell migration, which leads to the conclusion that alginate gel is a promising material for use as an implant for peripheral nerve regeneration.<sup>47</sup>

#### 2.4.2.2.2. Chitosan

Chitin is the second most abundant polysaccharide found in nature and it can be isolated from the outer shell of crustaceans, insect exoskeletons, and fungal cell walls. As a biopolymer of N-acetyl-D-glucosamine monomeric units, chitin is extensively applied in a wide range of biomedical fields.<sup>1</sup>

Chitosan is a natural and hydrophilic copolymer of D-glucosamine and N-acetyl-D-glucosamine and it is obtained from full or partial N-deacetylation of chitin.<sup>1</sup> It is also considered as a mucopolysaccharide with structural characteristics similar to glycosamines.<sup>48</sup> Since chitosan and glycosaminoglycans have very similar molecular structure, there are interactions between this biopolymer and ECM molecules including laminin, fibronectin and collagen.<sup>28</sup> Its biodegradability, biocompatibility, non-antigenicity, notable affinity to proteins, promotion of cell adhesion and non-toxicity has made it possible to use chitosan in a number of biomedical applications, including wound dressings, drug delivery systems and space-filing implants.<sup>30,48</sup> It has also seen its application in the tissue engineering field increase largely, serving as a candidate biomaterial for the development of neural scaffolds.<sup>1</sup>

Being fragile in the dried form, chitosan can be chemically crosslinked or jointly used with other materials before scaffold fabrication.<sup>1</sup> Chitosan matrices have low mechanical strength under physiological conditions and are unable to maintain a predefined shape after transplantation.<sup>28</sup> For instance, their mechanical properties can be improved by modification with a silane agent named  $\gamma$ -glycidoxypropyltrimethoxysilane (GPTMS), which is one of the silane-coupling agents which has epoxy and methoxysilane groups. This modification, along with a freeze-drying technique, has been shown to produce chitosan type III membranes with 90% porosity and successful improvement of rat sciatic nerve regeneration after axonotmesis. It was concluded that this material, apart from working as a simple mechanical scaffold, could also work as an inducer of nerve regeneration.<sup>28,49,50</sup>

In another study, crystalline chitosan tubes with a tubular structure and an appropriate size for peripheral nerve reconstruction were obtained by removing calcium phosphate and proteins from crab tendons. Its mechanical strength however was low perpendicular to its longitudinal axis, resulting in the swelling of the tube surface wall which caused stenosis.<sup>51</sup> To improve the mechanical properties of a chitosan tube one can heat-press it into a triangular shape and modify it into apatite using an alternate soaking method.<sup>52</sup>

Since it is considered a material with such good biomedical properties, several investigators have studied chitosan by testing it for peripheral nerve regeneration. It can be

fabricated using different techniques and it can be implanted with different forms, depending on the application site.

### 2.4.2.3. Synthetic Materials

Synthetic polymers constitute another class of promising biomaterials for fabricating neural scaffolds due to their tunable chemical and physical properties. However, these materials are incompatible with cell adhesion and tissue repair. Thus, they are often modified to render them “cell friendly.”<sup>1</sup>

Silicone tubes represent one of the first and most frequently used NGCs prepared with non-degradable synthetic materials because of its inert and elastic properties. Despite its non-degradability and no permeability to large molecules, silicone tubes provide an important model system for studying nerve regeneration under controlled conditions and have been applied in clinical trials to bridge short nerve gaps with some success.<sup>1</sup>

Other non-degradable scaffolds have also been fabricated using acrylic polymer, polyethylene, and elastomer. Unfortunately, non-degradable materials are left in situ as foreign bodies after nerve regeneration, and therefore cause a chronic foreign body reaction with excessive scar tissue formation, ultimately inhibiting nerve functional recovery.<sup>1</sup>

In order to overcome the restrictions imposed by the non-degradable materials, many experiments have been conducted using biodegradable synthetic polymers such as polylactic acid (PGA), poly(L-lactic acid) (PLLA), poly(L-lactic-co-glycolic acid) (PLGA) and polycaprolactone (PCL), which are used to prepare neural scaffolds. These degrade within a reasonable time span, and the degradation products are absorbed by the body accompanied with mild foreign body reactions.<sup>1,4</sup>

Some of these synthetic materials properties can be modulated and tailored to match different application requirements and even to enable the entrapment of support cell or bioactive molecules for controlled delivery during nerve regeneration.<sup>1</sup> For example, in one study, previously tested PLLA conduits were used to enhance the efficacy of peripheral nerve regeneration by incorporating them with allogeneic Schwann cells.<sup>53</sup>

Of these materials, nerve guide implants made of collagen, PGA and poly-DL-lactide-co-caprolactone (PLCL) are now approved by the FDA for human application and are already in clinical use.<sup>4</sup>

## 2.5. Nerve Scaffold Functionalization

As mentioned before, NGCs can be functionalized depending on the desired application. Focal application of neurotrophic factors and cell transplantation are two examples of functionalization.<sup>5</sup>

### **2.5.1. Neurotrophic Factors**

Being a class of growth factors, neurotrophic factors can help to stimulate and control neurogenesis. They may be interchangeably termed as neurotrophins, but in its strict meaning, it only covers four structurally related factors: nerve growth factor (NGF), brain-derived neurotrophic factor (BDNF), neurotrophin-3, and neurotrophin-4/5. Neurotrophic factors have been widely investigated due to their role in nerve regeneration and their influence in neural development, survival, outgrowth and branching.<sup>1,54</sup>

Some neurotrophins such as the ciliary neurotrophic factor, the basic fibroblast growth factor and the BDNF are upregulated in Schwann cells in the degenerating axon segment. These neurotrophic factors can influence different functional classes of axons such as sensory and motor fibers, which makes essential to research and better understand the timing of expression and precise role of these factors in axonal regeneration, so this process can be enhanced.<sup>5</sup>

Understanding the changes that occur in growth factor expression in the injured peripheral nerve might indicate suitable pharmacological therapies for repair and enhancement of muscle reinnervation.<sup>55</sup> The NGF was the first neurotrophic factor to be identified and although it exists only in low levels in the healthy nerve, it shows rapid increases in expression after nerve injury. Satellite glial cells surrounding the dorsal root ganglion have been shown to up-regulate levels of NGF after axotomy, which contributes to the induction of sympathetic nerve sprouting after injury. Schwann cells at the injury site can also rapidly up-regulate NGF levels, possibly to compensate for the loss of supply from the nerve itself.<sup>55</sup> The BDNF has its origin in inflammatory cells and it has been demonstrated that it mediates neuroprotective effects. This is an important factor for motor neurons, influencing the expression of cholinergic genes and promoting cell survival in culture.<sup>16</sup>

However, in vivo responses to neurotrophic factors can vary due to the method of their delivering. Therefore, the development and use of controlled delivery devices are required for the study of complex systems.<sup>54</sup>

### **2.5.2. Support Cells**

Adding supportive cells to NGCs are one of the most extensively investigated modifications to the single-lumen nerve tube. One of the cell types is Schwann cells which are known to possibly enhance nerve regeneration by different mechanisms.<sup>29</sup> Schwann cells are a highly preferred substrate for axon migration and they also express neural cell adhesion molecules. Apart from Schwann cells, stem cells have been isolated from different regions of the human body and have been studied as candidates of support cells for nerve regeneration applications.<sup>15</sup>

### 2.5.2.1. Mesenchymal Stem Cells

Stem cells are a very unique cell type and have special characteristics that allow them to fulfil some functions that other cells cannot. Cell transplantation of mesenchymal stem cells (MSCs), embryonic stem cells (ESCs) and marrow stromal cells has been proposed as a method of improving peripheral nerve regeneration.<sup>7</sup> The success of their implantation depend on the fact that they can grow and divide indefinitely, can differentiate into specialized cells and be delivered to the site of lesion associated to biomaterials.<sup>30</sup>

Besides cell-based therapies for various diseases, MSCs have become one of the most interesting targets for tissue regeneration including peripheral nerves.<sup>1</sup> According to the International Society of Cell Therapy, MSCs are progenitor cells for the mesenchymal lineages, plastic adherent and also capable of self-renewal with sustained proliferation *in vitro* and can differentiate into multiple mesodermal cells, including neuron-like cells.<sup>7,27,30</sup> It is also possible for them to differentiate into non-mesenchymal lineages, including myelinating cells of the PNS. One of the advantages of using these cells is their high plasticity and low immunogenicity, which makes them a desirable form of cell therapy for the injured nervous system without requiring the use of immunosuppressive drugs during the treatments.<sup>7</sup>

MSCs have been isolated from various sources including skin, hair follicles, periosteum, amniotic fluid, umbilical cord, dental pulp and adipose tissue.<sup>7</sup> They can be harvested after birth, cryogenically stored, thawed and expanded for therapeutic uses.<sup>30</sup> Stem cells derived from extra-embryonic tissues are a good alternative to those derived from the umbilical cord, which have associated to them a painful aspiration.<sup>27</sup> MSCs isolated from the human umbilical cord matrix, also known as Wharton's jelly, are originated from inner cell mass of blastocyst and present positive effects in nerve and skeletal muscle regeneration being that there are no ethical or technical issues.<sup>28,30</sup> Comparing with ESCs, MSCs have shorter population doubling time, they can be easily cultured in plastic flasks and are well tolerated by the immune system which means that their transplantation into non-immune suppressed animals does not induce acute rejection. Also, they can differentiate into adipocytes, osteoblasts, chondrocytes, cardiomyocytes, neurons, and glia.<sup>27,30</sup>

Recently, stem cells derived from dental pulp (DPSCs) received growing attention due to common characteristics with other mesenchymal stem cells beside their ease of obtainment and propagation, since they can be isolated with non-invasive procedures. The use of DPSCs in research and therapy is therefore not considered to be controversial.<sup>56,57</sup> These cells can be successfully cryopreserved with good viability and function upon thawing, suggesting that it may be feasible to bank them and/or dental tissue.<sup>58</sup> Studies show that DPSCs could differentiate into many types of lineages, such as odontoblasts, osteoblasts, adipocytes, skeletal and smooth muscle cells, elastic cartilage cells, endothelial and neural cells both *in vivo* and *in vitro* conditions.<sup>56</sup>

There are two main techniques to implant cultured cells into defective nerves which have been subjected to either neurotmesis or axonotmesis. In the first case, the neural scaffold is interposed between the nerve stumps, being the cells injected directly into the scaffold. In

the axonotmesis case, the neural scaffold is placed around the crush injury. The cellular system can also be pre-added to the scaffold via injection or co-culture, being later implanted in the injured nerve.<sup>27</sup>

Contrarily to what happens with the fabrication of the neural scaffolds, the quality of cells varies within patients and it depends on the individual tissue characteristics, on the transport conditions and time of the samples to the laboratory and on the processing and cryopreservation techniques.<sup>27</sup>

## 2.6. Additional approaches

Besides all the strategies to regenerate peripheral nerves that are being studied, some others might be useful to complement or even improve them.

In some situations it may be of interest to use drug delivery systems made up of degradable biomaterials, which may become a helpful strategy for controlled release of growth factors.<sup>1</sup> Furthermore, a study has shown that the ability of an artificial nerve guide to deliver growth factors and Schwann cells is important for enhancing functional recovery.<sup>55</sup> In these cases, degradable grafts are advantageous because, as they degrade, they will release growth or trophic factors trapped in or adsorbed to the polymer.<sup>4</sup>

In addition, electric stimulation has been shown to enhance nerve regeneration, and thereby construction of tissue engineered nerve grafts with electrically conductible polymers or by nanotechniques may represent some new avenues worthy of intensive research.<sup>1</sup>

Transplantation of Schwann cells could assist the regenerative process in a way that they can be added directly to the lumen of a biodegradable artificial nerve graft.<sup>12</sup> Because they can be grown relatively easily in culture, they can be manipulated to enhance their regenerative properties or to act as vehicles for gene therapy.<sup>10</sup> Schwann cells suspended in gelatin within the lumen of a PGA acid conduit have been shown to support nerve regeneration over a 30-mm gap in the peroneal nerve in rabbits.<sup>12</sup>

Hydrogels are water-swollen crosslinked polymer networks that often present characteristics such as tissue-like elasticity and mechanical strength.<sup>59</sup> They are used in clinical and experimental practice in various applications, including tissue engineering. Hydrogels are usually considered highly biocompatible due to their high water content and also to the physiochemical similarity with the native ECM. Dextrin, a starch-based natural polymer, has a great potential for the development of hydrogels owing to its proven clinical tolerability and efficient absorption. This low molecular weight polymer was used to develop a resorbable hydrogel without using any chemical initiators. Dextrin was oxidized with sodium periodate and after testing it showed good mechanical properties and biocompatibility. It presents a three-dimensional network with a continuous porous structure which can be used to fill the lumen of NGCs.<sup>60,61</sup>

## Chapter 3

# Preliminary Experimental Work

This section outlines the preliminary work performed as a preparation for the dissertation experimental work and it was a task developed in a financed project of the laboratory - QREN I&DT Cluster in Development of Products for Regenerative Medicine and Cell Therapies - Projects Biomat & Cell QREN 2008/1372, co-financed by the European Community FEDER fund through ON2 - O Novo Norte - North Portugal Regional Operational Program 2007-2013, by project FCT "Hybrid Nanostructured Hydrogels: Bone regeneration using Multifunctional injectable Hydrogels - Rebone" - ENMED/0002/2010 from Fundação para a Ciência e Tecnologia (FCT). Also these results were obtained in collaboration with other researchers of the referred project.

### 3.1 Culture of Mesenchymal Stem Cells

The culture procedure of one of the cellular systems - MSCs from the Wharton's jelly of the umbilical cord - has been already tested associated to several biomaterials in the axonotmesis and neurotmesis injury model, and by me for the proposed thesis.<sup>27,62</sup>

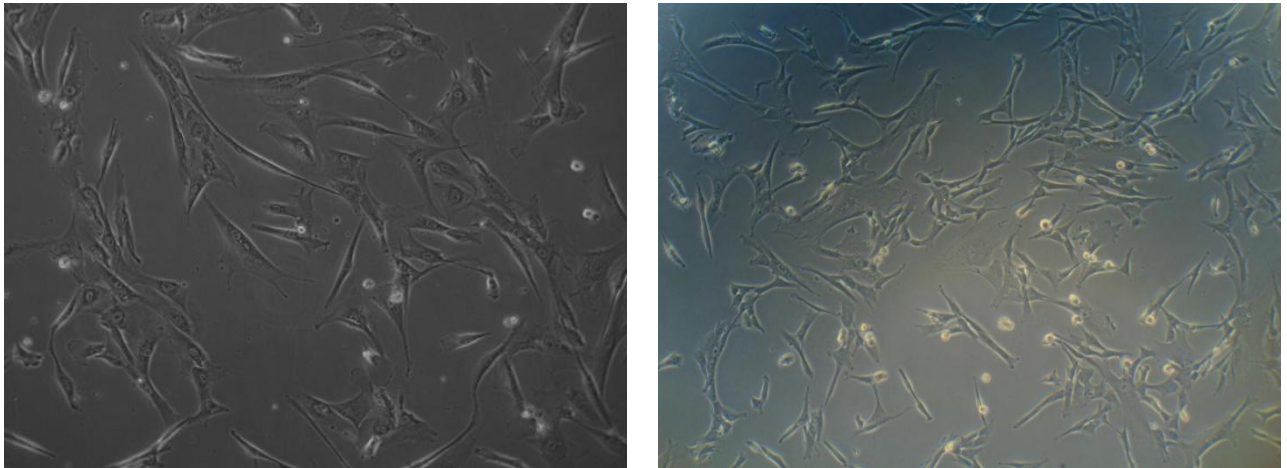


**Figure 4** - MSCs from Wharton's jelly exhibiting a mesenchymal-like shape with a flat polygonal morphology (left). After 72h of culture in neurogenic medium the cells became exceedingly long and there is a formation of typical neuroglial-like cells with multibranches (right) (x100).

Figure 4 represents the morphology of MSCs derived from Wharton's jelly in culture. MSCs were expanded and exhibited a mesenchymal-like shape with a flat and polygonal morphology. During expansion the cells became long spindle-shaped and colonized the whole culturing surface.

Before *in vivo* testing, cells were also characterized by flow cytometry analysis for a comprehensive panel of markers, such as platelet endothelial cell adhesion molecule - 1 (PECAM-1, CD31), homing cell adhesion molecule (HCAM, CD44), CD45, and Endoglin (CD105). The MSCs phenotype was confirmed and also the karyotype analysis was performed to confirm the somatic and sexual chromosome stability.

### 3.2 Animal Model

In this manuscript, it is briefly resumed the results already obtained with the evaluation of the biocompatibility of the cellular system and a hydrogel that can be used as a vehicle in axonotmesis and neurotmesis injuries reconstruction and that might improve the healing process.

Concerning the test performed in rats, for the *in vivo* subcutaneous implantation a total of 34 rodents were used. The adult male Sasco Sprague Dawley rats (Charles River Laboratories, Barcelona, Spain) weighed from 250 to 300 g and were randomly divided into groups of three animals each. Two animals were housed per cage in approved ones (Makrolon Type 4, Tecniplast, VA, Italy), in a room with controlled temperature and humidity with light and dark cycles every 12 hours. The animals were allowed normal cage activities under standard laboratory conditions and were fed with standard chow and water *ad libitum*.

All the animal testing procedures were in conformity with the Directive 2010/63/EU of the European Parliament and with the approval of the Veterinary Authorities of Portugal in

accordance with the European Communities Council Directive of November 1986 (86/609/EEC). Humane endpoints were followed in accordance to the OECD Guidance Document on the Recognition, Assessment and Use of Clinical Signs as Humane Endpoints for Experimental Animals Used in Safety Evaluation (2000). Adequate measures were taken to minimize pain and discomfort considering humane endpoints for animal suffering and distress. Animals were housed for two weeks before entering the experiment.

### 3.3 Experimental Procedure

Anesthesia was achieved with an intraperitoneal injection of a pre-mixed solution consisting of 100 mg/kg of body weight of ketamine (Imalgène 1000<sup>®</sup>) and 200 mg/kg of body weight of xylazine (Rompun<sup>®</sup>). Hair from the dorsal area of the animals was clipped and the skin scrubbed in a routine fashion with an iodopovidone 10% solution (Betadine<sup>®</sup>) and three long incisions of about 1,5-2 cm were made. Incision 1 was left-cranial, incision 2 was mid-right and incision 3 was left-caudal. To rat number three of each experimental group was performed a fourth type of incision, which was near the tail, corresponding to sham sample. After blunt dissection towards the ventral aspect of the body, the biomaterials were deposited subcutaneously. Skin and subcutaneous tissues were closed with a simple-interrupted suture of a non-absorbable filament (Synthofil<sup>®</sup>, Ethicon). After the experimental period, samples were collected on days 3 and 15. Afterwards, the rats were euthanized by lethal intracardiac injection of 5% sodium pentobarbital (Euthasil<sup>®</sup>). The implant area was then excised, with limits large enough to also retrieve sufficient unaffected surrounding tissue.

As described before, dextrin hydrogel was obtained through oxidation by sodium periodate and then cross-linked with adipic acid dihydrazide. The sterilization of dextrin hydrogels was performed by gamma radiation (room temperature; 25 kGy). Immediately before implantation, the hydrogel was crosslinked and allowed complete full gelation inside a syringe for administration. The hydrogel was developed by the research group from Universidade do Minho, supervised by Prof. Miguel Gama and included in the PhD thesis of Dr. Dina Silva.

### 3.4 Samples analysis

After collecting the samples, a macroscopic evaluation was performed followed by photographic records. Each implant site was examined for alterations in the normal structures, the nature and extent of any tissue reaction such as hematoma, edema, encapsulation and/or additional gross findings and for the presence, form and location of implant including possible remnants of degradable materials. Whenever possible, lymph nodes from the rat were also collected in order to assess for material migration and other abnormalities. However, collecting the lymph nodes might prove very difficult when no enlargement is present, due to the size of the test animals.



Macroscopic evaluation of the samples allowed the observation that all the tissue surrounding the implant zone did not exhibit signs of abnormalities or infection. Furthermore, there were no signs of fibrous capsule formation around the materials implanted. Hydrogel samples were still possible to identify after three days post-implantation as seen in Figure 5. This result indicates that the hydrogel degradation rate *in vivo* is lower than *in vitro*.

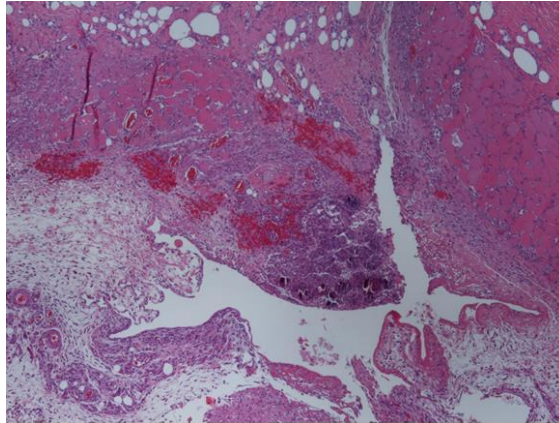


Figure 5 - Hydrogel after 3 days.

For the sample which contained the hydrogel and MSCs, the quantity of hydrogel that remained in the implant site was smaller when compared with the hydrogel alone (Figure 6). This may be explained by the dilution that occurred during the incorporation of MSCs in the hydrogel mixture, which affects the crosslinking reaction.

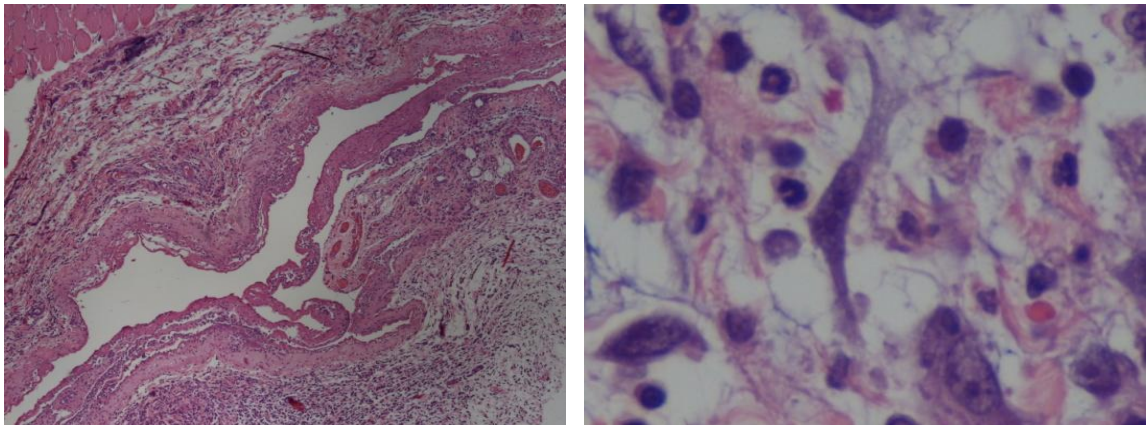


Figure 6 - MSCs and hydrogel after 3 days.

Sample collection after 15 days showed that no hydrogel sample was present in the implant site, as seen in Figure 7.

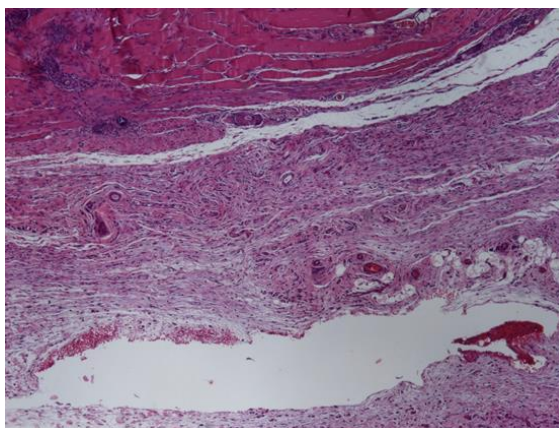


Figure 7 - Hydrogel after 15 days.

In cases when animals presented signs of ill health or reactions to the implant, a gross necropsy and collection of other organs were indicated to assess systemic toxicity. All the observed organs (kidney, liver, spleen and lungs) from these experimental animals presented normal characteristics and, despite being subjected to proper histological processing, they have not yet been evaluated.

### 3.5 Histological study

To perform the microscopic evaluation of the tissue response, two kinds of scoring systems have been reported and are classified as quantitative and semi-quantitatively scoring systems. In the case of this study, a semi-quantitative system was adopted, following the suggestion on the Annex E of the ISO 10993-6 standard. Such system was preferred over more recent references as these have not yet been validated for all of the test species and evaluated tissues the work group routinely deals with.

The collected samples were fixed using 10% buffered formalin and processed for routine histology. The first important microscopic aspect observed was that the lesion and the traces of the implants were located below the muscle layer rather than at the subcutaneous area. This may be due to the movement of the animal, which made the implant to shift to the lower layer.

Table 1 - Histological scoring.

TEST SAMPLE 3 days	SCORE (TEST-SHAM)	CLASSIFICATION
Hydrogel	4,05	SLIGHT IRRITANT
Hydrogel + MSCs	2,45	NON-IRRITANT
TEST SAMPLE 15 days	SCORE (TEST-SHAM)	CLASSIFICATION
Hydrogel	2,14	NON-IRRITANT
Hydrogel + MSCs	0	NON-IRRITANT

### **3.6 Final considerations**

After the analysis of the histological results, it was possible to assess various key parameters to determine the local effect of the implanted material such as the extent of fibrosis/fibrous capsule and inflammation, the degeneration, the number and distribution of the inflammatory cell types, such as polymorph nuclear neutrophilic leucocytes, lymphocytes, plasma cells, eosinophils, macrophages and multinucleated cells, the presence, extent and type of necrosis, the vascularization, fatty infiltration, granuloma and bone formation and fragmentation and/or debris presence, form and location of remnants of degraded material.

Based on the preliminary results obtained, some provisory conclusion can be pointed out. The dextrin hydrogel seemed to elicit only a slightly irritant acute response, which tends to evolve favorably. Therefore, this hydrogel appears to be a suitable vehicle for implantation. Also, the inclusion of MSCs to the system seemed to induce a positive effect on the progression of the inflammatory response. The acute tissue response appeared to be more controlled and to be evolving faster towards the confinement of the lesion within a fibrous capsule.

## Chapter 4

# Experimental Work

This section outlines all the experimental work performed and respective display and interpretation of results.

The goals established for this work were to prepare chitosan guide tubes crosslinked with GPTMS, to mechanically and structurally characterize them, and finally to implant them in a group of animals. This would allow to compare the obtained results with others already described and published and to assess if improvements were achieved.

### 4.1 Materials and Methods

#### 4.1.1. Preparation of the guide tubes

Chitosan (degree of deacetylation: >75%; Sigma-Aldrich<sup>®</sup>, USA) was dissolved at room temperature in a 0.25 M acetic acid solution in order to attain a concentration of 2% (w/v). At the same time, GPTMS (Sigma-Aldrich<sup>®</sup>, USA) was also dissolved for 1 h at room temperature in a 0.25 M acetic acid solution, resulting in a concentration of 27.7% (w/v). In order to induce the crosslinking, the GPTMS solution was added to the chitosan solution to obtain a molar ratio of 1:0.5 (chitosan:GPTMS). After stirring at room temperature for 1 h, the resultant chitosan-GPTMS solution was poured into teflon molds which were kept at -20°C for 24 h. The frozen guide tubes were subsequently transferred to a freeze-dryer (FreeZone Plus 2.5 Freeze Dry System, Labconco<sup>®</sup>, USA) in which the samples were lyophilized for 48 h to complete dryness. These guide tubes were then soaked in a 0.1 M NaOH aqueous solution to neutralize remaining residues of acetic acid, carefully washed with distilled water, and lyophilized once again for another 48 h. In the end of the preparation, the guide tubes were 1.6 cm long, had an internal diameter of 3 mm and a wall thickness of 1.5 mm. Finally, the guide tubes were stored until being used for implantation and other assays.<sup>8,49,62,63</sup>

PLGA guide tubes were also prepared in order to make a comparison between them and chitosan-GPTMS guide tubes. PLGA copolymers with a ratio of 90(PLA):10(PLG) were obtained

from their cyclic dimmers, DL-lactide and glycolide. Synthetic nonwoven constructs were used to prepare the guide tubes. These materials are extremely flexible, biologically safe, and are able to sustain the compressive forces due to body movement after implantation.<sup>64,65</sup>



**Figure 8** - Chitosan-GPTMS (left) and PLGA (right) guide tubes before implantation.

#### **4.1.2. Structural characterization of the guide tubes**

##### **4.1.2.1. Scanning Electron Microscopy (SEM)**

The morphology and microstructure of the chitosan-GPTMS guide tubes were observed under a scanning electron microscope (Quanta 650, FEI™, USA) with an accelerating voltage of 5 kV. Previous to observation, the samples were coated with a thin gold layer using a sputter coating (Polaron SC502).

##### **4.1.2.2. Fourier Transform Infrared (FTIR) Spectroscopy**

Chitosan-GPTMS guide tubes and chitosan powder were characterized by FTIR spectroscopy. Infrared spectra were obtained by an infrared spectrometer (Jasco® 4100). 64 scans were performed with a resolution of 4 cm<sup>-1</sup>.

##### **4.1.2.3. Water uptake assay**

In order to evaluate the water uptake of the guide tubes, the samples were soaked in a phosphate-buffered saline (PBS) solution at pH 7.4. Samples were weighed in their dry form and then kept at 37°C. The ratio between their masses and the volume of PBS had to be at least of 1:10 (w/v). After each time point the samples were left to dry on top of a filter paper and then weighed and put in a new solution of PBS. This way the water uptake was obtained, i.e., the amount of water adsorbed according to Equation 1, where  $W_d$  and  $W_w$  stand for the weights of the guide tubes before and after being soaked in PBS, respectively.<sup>48</sup>

$$\text{Water uptake (\%)} = \frac{W_w - W_d}{W_d} \times 100 \quad (1)$$

#### 4.1.2.4. Determination of the degree of crosslinking

The degree of crosslinking of the guide tubes was evaluated by ninhydrin (NHN) assay, which determines the percentage of free amino groups (NH<sub>2</sub>) remaining in the guide tubes after crosslinking. At first, a solution of citric acid, NaOH 1.0 M and SnCl<sub>2</sub>·2H<sub>2</sub>O was prepared and mixed for 45 minutes with a solution of ninhydrin dissolved in ethylene glycol monomethyl ether. Then, a sample was heated to 100°C in a water bath with 1 mL of ninhydrin solution for 20 minutes. The solution was cooled down to room temperature, diluted with 50% isopropanol, and then its optical absorbance was measured at 570 nm with a spectrophotometer (UV-2501PC, Shimadzu). The optical absorbance of the chitosan powder was also measured at 570 nm. The amount of free amino groups in the test sample is proportional to the optical absorbance of the solution. The concentration of free amino groups in the sample was determined from a calibration curve of glycine concentration vs absorbance. The concentration measured was divided by sample weight, and multiplied by the sample molecular weight to obtain the mole NH<sub>2</sub>/mole sample. The degree of crosslinking of the sample was then calculated according to Equation 2, where NHN reactive amine<sub>fresh</sub> is the mole fraction of free NH<sub>2</sub> in non-crosslinked samples and NHN reactive amine<sub>fixed</sub> is the mole fraction of free NH<sub>2</sub> remaining in crosslinked samples.<sup>66</sup>

$$\% \text{Degree of crosslinking} = \frac{\text{NHN reactive amine}_{\text{fresh}} - \text{NHN reactive amine}_{\text{fixed}}}{\text{NHN reactive amine}_{\text{fresh}}} \times 100 \quad (2)$$

#### 4.1.2.5. Mechanical assay

In order to evaluate the mechanical behaviour of the guide tubes, stress-strain curves were recorded using dry and hydrated samples. The latter were kept for 2 h in ultra pure water. Strip-shaped membranes were stretched using a crosshead speed of 1 mm.min<sup>-1</sup> (AG-IS 500N, Autograph, Shimadzu). Five samples for each condition were tested. The Young modulus (E) was calculated from the stress at break and the strain at break of the guide tubes.



Figure 9 - Chitosan-GPTMS membrane assembled in the universal testing machine.

### 4.1.3. *In vivo* Testing

#### 4.1.3.1. Ethics and Regulation

All the animal testing procedures were in conformity with the Directive 2010/63/EU of the European Parliament and with the approval of the Veterinary Authorities of Portugal in accordance with the European Communities Council Directive of November 1986 (86/609/EEC). Humane end points were followed in accordance to the OECD Guidance Document on the Recognition, Assessment and Use of Clinical Signs as Humane Endpoints for Experimental Animals Used in Safety Evaluation (2000). Adequate measures were taken to minimize pain and discomfort taking into account humane endpoints for animal suffering and distress. Animals were housed for two weeks before entering the experiment.

#### 4.1.3.2. Microsurgical Procedure

Adult male Sasco Sprague Dawley rats (Charles River Laboratories, Barcelona, Spain) weighing between 250 and 300 g were used for the *in vivo* tests and randomly divided in groups of 6 animals each for control groups (*Gap*, *End-to-end*, *Graft*, *PLGA* and Chitosan-GPTMS (*Ch-GPTMS*) groups). The *Ch-GPTMS* group with a neurotmesis injury surgically reconstructed with a chitosan guide tube was only composed by 4 animals. All animals were housed in a temperature and humidity controlled room with 12-12 h light/dark cycles and



were allowed normal cage activities under standard laboratory conditions. The animals were fed with standard chow and water *ad libitum*.

For surgery, the animals were placed prone under sterile conditions and the skin from the clipped lateral right thigh was scrubbed in a routine fashion with antiseptic solution. Rats were put under deep anaesthesia (ketamine 90 mg/kg; xylazine 12.5 mg/kg, atropine 0.25 mg/kg, intraperitoneal), after which the right sciatic nerve was exposed through a skin incision extending from the greater trochanter to the mid-thigh distally followed by a muscle splitting incision. After nerve mobilization, all animals were subjected to a transection injury (neurotmesis) immediately above the terminal nerve ramification using straight microsurgical scissors. Then, the proximal and distal nerve stumps were inserted into the guide tube which was held in place with 2 epineurial sutures using 7/0 monofilament nylon. Opposite leg and sciatic nerve were left intact in all animals (*Ch-GPTMS* group - Group 6). A group of 6 animals was used as control without any sciatic nerve injury (Group 1 - *Control*). In Group 2 the injured nerve was left without any repair intervention (Group 2 - *Gap*). In Group 3, immediate coaptation with 7/0 monofilament nylon epineurial sutures of the 2 transected nerve endings was performed (Group 3 - *End-to-End*). In Group 4 (Group 4 - *Graft*), the sciatic nerve was transected immediately above the terminal nerve ramification and at a 10 mm distal point. The nerve graft obtained, with a length of 10 mm was inverted 180° and sutured with 7/0 monofilament nylon. Opposite leg and sciatic nerve were left intact in all groups and served as control for normal nerves. Finally, in Group 5 (Group 5 - *PLGA*), after transection of the sciatic nerve, both the proximal and distal nerve stumps were inserted 3 mm into a PLGA guide tube and held in place with 2 epineurial sutures using 7/0 monofilament nylon.

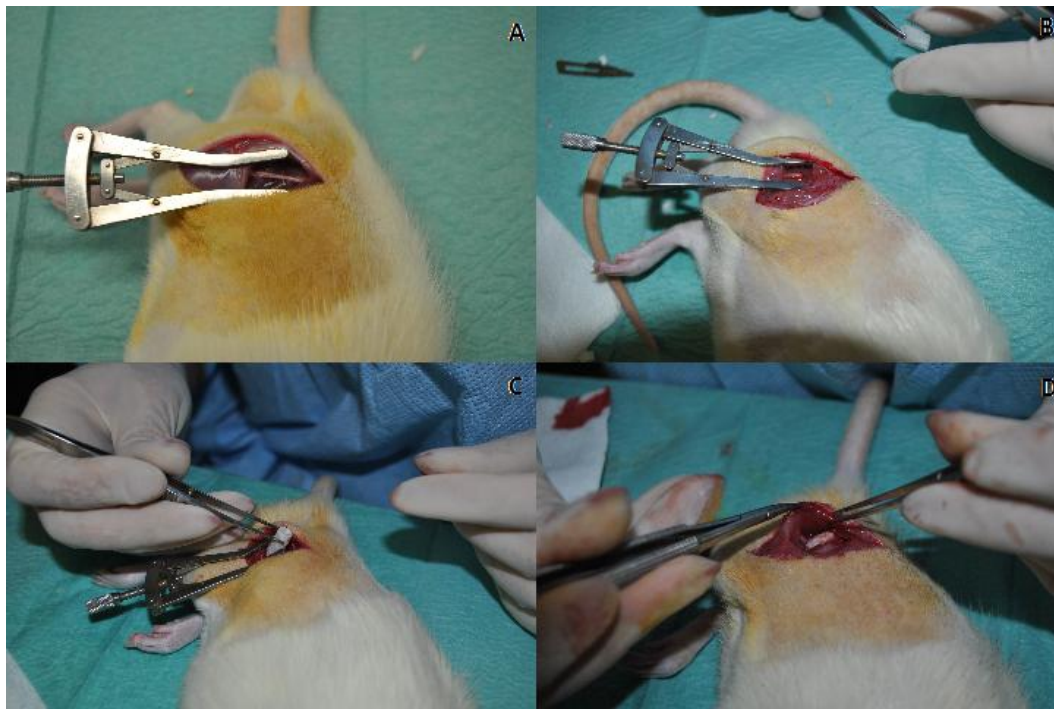


**Figure 10** - Rat sciatic nerve before (A) and after neurotmesis (B), followed by the nerve reconstruction with a chitosan-GPTMS guide tube (C and D).



### 4.1.3.3. Functional Assessment

All animals were tested pre-operatively (week 0), at week 1 and every two weeks after the surgery, for a total period of follow-up of 20 weeks. Animals were gently handled and tested in a quiet environment to minimize stress levels.

#### 4.1.3.3.1. Evaluation of Motor Performance and Nociceptive Function

Motor performance and nociceptive function were evaluated by measuring extensor postural thrust (EPT) and withdrawal reflex latency (WRL), respectively.

The EPT test was proposed as a part of the neurological recovery evaluation in the rat after sciatic nerve injury.<sup>67</sup> For this test the entire body of the rat, except for the hindlimbs, was wrapped in a surgical towel. Supporting the animal by the thorax and lowering the affected hindlimb towards the platform of a digital balance, the EPT was elicited. As the animal is lowered to the platform, it extends the hindlimb, anticipating the contact made by the distal metatarsus and digits. The force applied in grams by the rat towards the digital balance was recorded. The same procedure was applied to the contra-lateral, unaffected limb. For this test, both limbs were tested 3 times and the 3 values were averaged in order to obtain a final result. The normal EPT (NEPT), regarding the unaffected limb, and the experimental EPT (EEPT) values were incorporated into Equation 3 to derive the percentage of functional deficit.<sup>64,68,69</sup>

$$\% \text{ Motor deficit} = \frac{NEPT - EEPT}{NEPT} \times 100 \quad (3)$$

The hotplate test previously described in the literature was modified to assess the nociceptive withdrawal reflex.<sup>70</sup> Wrapped in a surgical towel, the animal was positioned so it would stand with the affected hind paw on a plate at 56°C. WRL is defined as the time elapsed from the onset of hotplate contact to withdrawal of the hind paw and measured with a stopwatch. Normal animals withdraw their paws from the hotplate within 4.3 seconds or less.<sup>49,64,71</sup> Both the affected and normal limbs were tested 3 times and the three latencies were averaged to obtain a final result. If there was no paw withdrawal after 12 seconds, the heat stimulus would be ceased in order to prevent tissue damage, and the animal would be assigned the maximal WRL of 12 seconds.

#### 4.1.3.3.2. Sciatic functional index and static sciatic index

For sciatic functional index (SFI), the animals were tested in a confined walkway measuring 42 cm long and 8.2 cm wide, with a dark shelter at the end.<sup>64,72,65</sup> White paper sheets were placed on the floor of the walkway. The hind paws of the rats were pressed down onto a finger paint-soaked sponge, after which they were put to walk down the corridor leaving its hind footprints on the paper. Several measurements were taken from the

footprints: (i) distance from the heel to the third toe, the print length (PL); (ii) distance from the first to the fifth toe, the toe spread (TS); and (iii) distance from the second to the fourth toe, the intermediary toe spread (ITS). For both dynamic (SFI) and static assessment (SSI), all measurements were taken from the experimental (E) and normal (N) hindlimbs. Prints for measurements were chosen at the time of walking based on clarity and completeness at a point when the rat was walking briskly. The mean distances of the three measurements were used to calculate the following factors (dynamic and static):

$$\text{Toe spread factor (TSF)} = \frac{ETS-NTS}{NTS} \quad (4)$$

$$\text{Intermediate toe spread factor (ITSF)} = \frac{EITS-NITS}{NITS} \quad (5)$$

$$\text{Print length factor (PLF)} = \frac{EPL-NPL}{NPL} \quad (6)$$

SFI was calculated as described in the literature according to Equation 7 and averaged values were used.<sup>73</sup>

$$\begin{aligned} SFI &= -38.3 \left( \frac{EPL-NPL}{NPL} \right) + 109.5 \left( \frac{ETS-NTS}{NTS} \right) + 13.3 \left( \frac{EIT-NIT}{NIT} \right) - 8.8 \\ &= (-38.3 \times PLF) + (109.5 \times TSF) + (13.3 \times ITSF) - 8.8 \end{aligned} \quad (7)$$

For the SSI evaluation, only the parameters TS and ITS were measured.<sup>74</sup>

$$SSI = [(108.44 \times TSF) + (31.85 \times ITSF)] - 5.49 \quad (8)$$

For both SFI and SSI, an index score of 0 is considered normal and an index of -100 indicates total impairment. When no footprints were measurable, an index score of -100 was given.<sup>75</sup>

#### 4.1.3.4. Sciatic nerve stereology and histological analysis

A histomorphometric analysis was performed for the present case study. Nerve samples obtained from un-operated controls were processed for quantitative morphometry of myelinated nerve fibers.<sup>76</sup> Fixation was carried out using 2.5% purified glutaraldehyde and 0.5% saccharose in 0.1 M Sorensen phosphate buffer for 6 to 8 h and resin embedding was obtained following Glauerts' procedure.<sup>77</sup> Series of about 50 semi-thin transverse sections (2  $\mu$ m thick) were cut using a Leica Ultracut UCT ultramicrotome (Leica Microsystems, Wetzlar, Germany) starting from the distal end of the specimen and stained by Toluidine blue. Stereology was carried out on one section, randomly selected each of these series, using a DM4000B microscope equipped with a DFC320 digital camera and an IM50 image manager system (Leica Microsystems, Wetzlar, Germany). Systematic random sampling and D-dissector

were adopted using a protocol previously described.<sup>78,79</sup> Fiber density and total number were estimated together with fiber and axon diameter and myelin thickness.

#### 4.1.4 Statistical analysis

Differences in motor deficit and nociception recoveries and axon counts between experimental groups were analyzed by two-way mixed factorial ANOVA, with experimental groups as between subjects factor, and time of recovery as the within subjects factor. Whenever a significant main effect was found for the between subjects factor, pairwise comparisons were carried out by applying the Turkey's HSD post hoc test. The Mauchly's test of sphericity was used to assess sphericity, and in cases significant deviations from the later existed, a correction of the degrees of freedom was used by means of the more conservative Grenhouse-Geiser's Epsilon. T tests were used for comparisons between experimental groups at week 1 post-surgery, with Bonferroni adjustment for multiple comparisons. All statistical analysis were carried out using the SPSS software package (SPSS, Chicago) and statistical significance was accepted at  $P < 0.05$ . The experimental *Ch-GPTMS* group was not included in this preliminary statistical analysis. It will be included in the end of the 20 week recovery period.

## 4.2 Results

### 4.2.1 SEM

Figure 11 shows the microstructure of the chitosan-GPTMS guide tubes, being that Figure 11(B) is a close-up of Figure 11(A). The images clearly show that the chitosan-GPTMS guide tubes are highly porous, which is in accordance to previous studies where investigators produced chitosan-GPTMS membranes also highly porous. In these studies, it was demonstrated that the membranes had a porosity of ~90% and that pores were  $110 \mu\text{m}$ .<sup>8</sup>

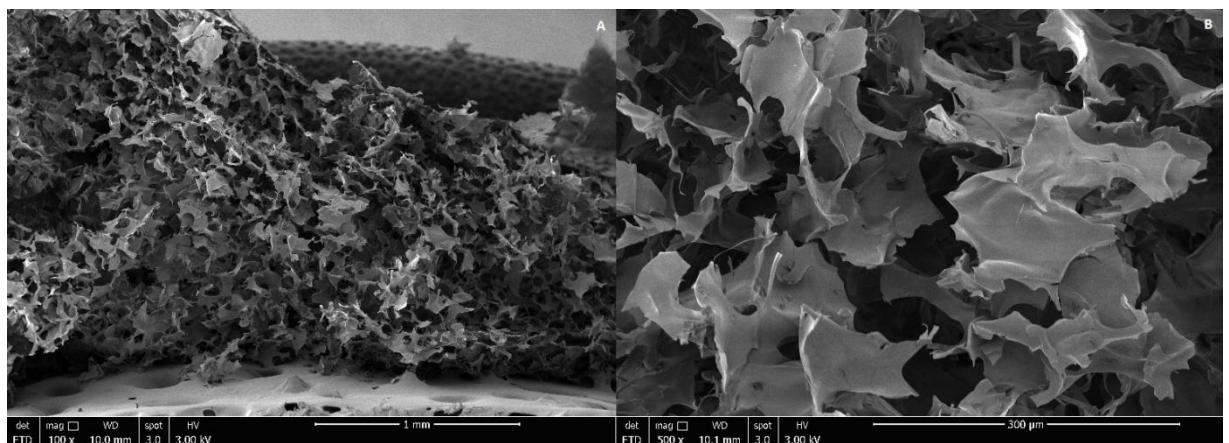


Figure 11 - SEM images of the chitosan-GPTMS guide tubes.

### 4.2.2 FTIR

The FTIR spectra of chitosan-GPTMS guide tubes and chitosan powder is represented in Figure 12(A) and Figure 12(B), respectively. The GPTMS monomer has three characteristic peaks at  $2840\text{ cm}^{-1}$ ,  $1192\text{ cm}^{-1}$  and  $914\text{ cm}^{-1}$ .<sup>80</sup> The bands around  $1650$  and  $1565\text{ cm}^{-1}$  are characteristic of chitosan and are denoted as amide bands I and II, respectively.<sup>81,82</sup> In the chitosan spectrum, the wide peak in the  $3500\text{-}3300\text{ cm}^{-1}$  region is attributed to hydrogen-bonded O-H stretching vibration. The peak for asymmetric stretch of C-O-C is found at around  $1150\text{ cm}^{-1}$  and the peak at  $1317\text{ cm}^{-1}$  corresponds to the C-N stretching vibration of type I amine.<sup>83</sup> The reaction between amine groups in chitosan and oxirane groups in GPTMS can be noticed in the transmittance band at  $1550\text{ cm}^{-1}$ .<sup>84</sup>

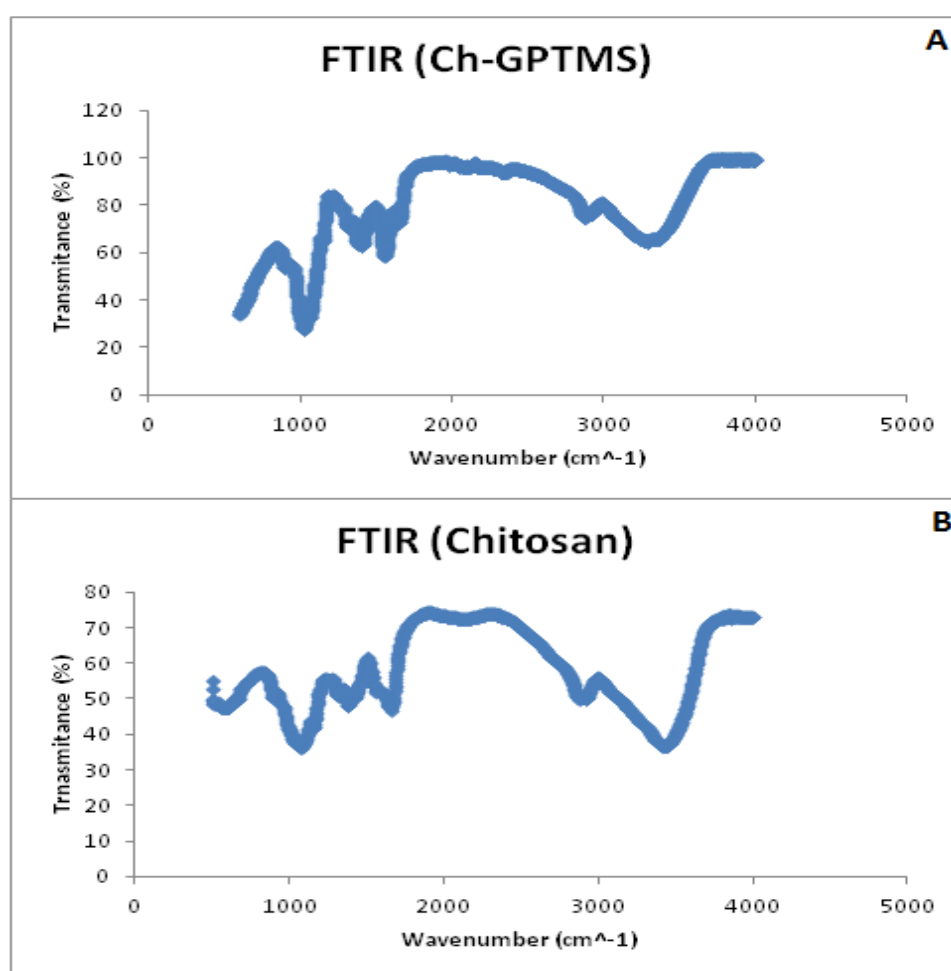


Figure 12 - FTIR spectrum of chitosan-GPTMS guide tubes (A) and chitosan powder (B).

### 4.2.3 Water uptake

Figure 13 shows the water uptake of the chitosan-GPTMS guide tubes throughout a period of 7 days during which they were kept at  $37^{\circ}\text{C}$  and completely immersed in the PBS solution

at pH 7.4. In the first two hours, the guide tubes quickly absorbed the fluids since the water uptake is nearly 1000% of the initial dry mass. After 24 hours, the water uptake of the guide tubes rises up to ~1400% and from this point on the water uptake decreases which may be due to mass loss.

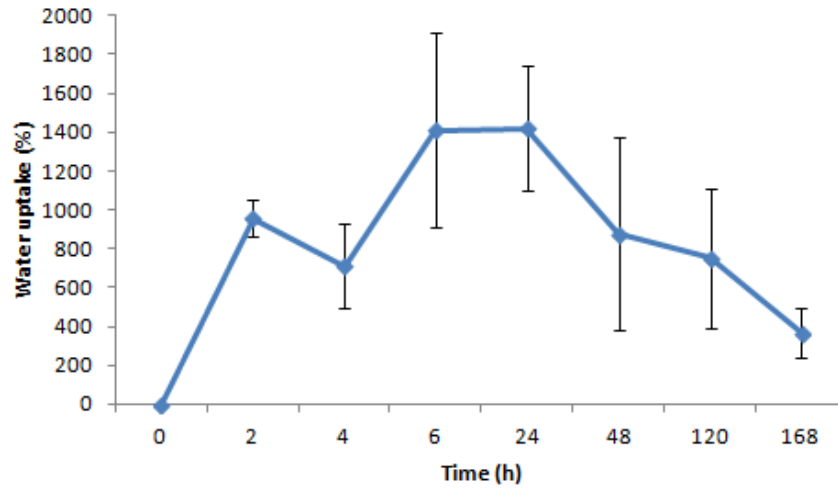


Figure 13 - Averaged values of water uptake (%) of the chitosan-GPTMS guide tubes as function of the period of soaking in PBS.

#### 4.2.4 Degree of crosslinking

As mentioned before, GPTMS was used in this study as a crosslinking reagent at the time of preparation of the chitosan-GPTMS guide tubes. Their degree of crosslinking was calculated by Equation 2 previously described and a degree of crosslinking around 69% was obtained for chitosan-GPTMS samples.

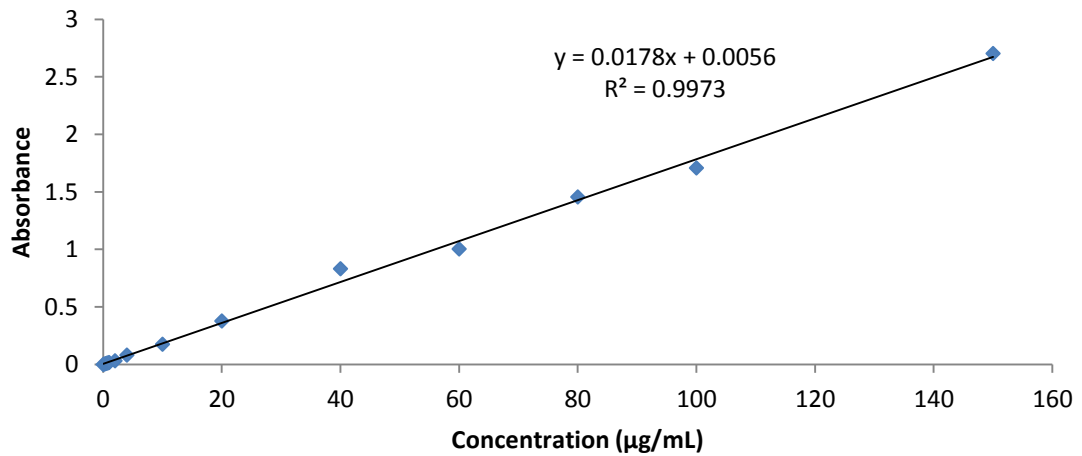


Figure 14 - Calibration curve of glycine.

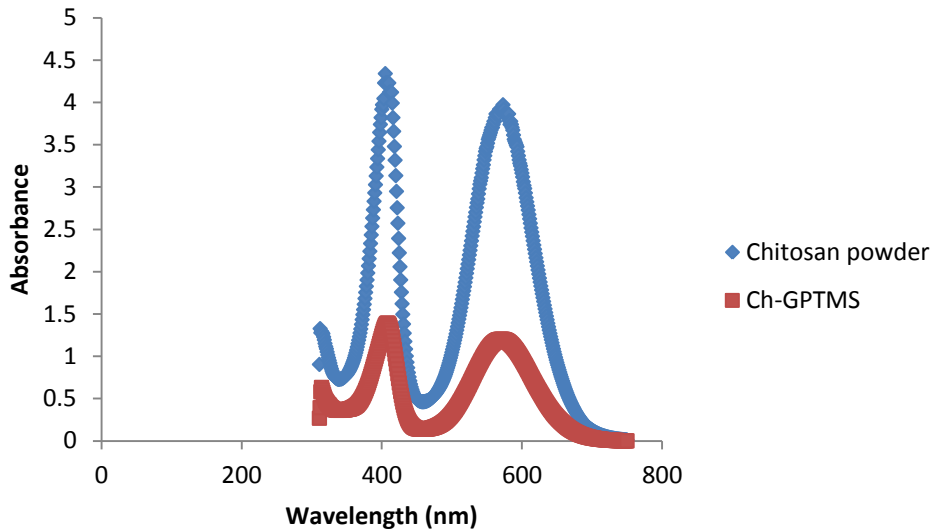


Figure 15 - Optical absorbance of the chitosan powder and the chitosan-GPTMS guide tubes.

#### 4.2.5 Mechanical assay

Dimensional stability and mechanical integrity of conduits are an important feature in tissue and biomedical engineering applications, because material often requires manipulation, and sample integrity must be maintained. In that sense, stress-strain curves were plotted and the Young modulus (E) calculated for both conditions at a fixed strain of 2% for dry and hydrated samples (Figure 16). It was observed that samples present an increase of the stress with increasing strain until material collapse occurs (Figure 17) Furthermore, hydrated samples present ultimate tensile stress lower than the one of the dry samples due to the amount of water that fills sample porous structure and probably works as a plasticizer agent, leading to a decrease of the Young modulus for the hydrated samples. Finally, the Young modulus of the hydrated samples (Table 2) summarizes the mechanical results obtained for chitosan samples in dried and hydrated states.

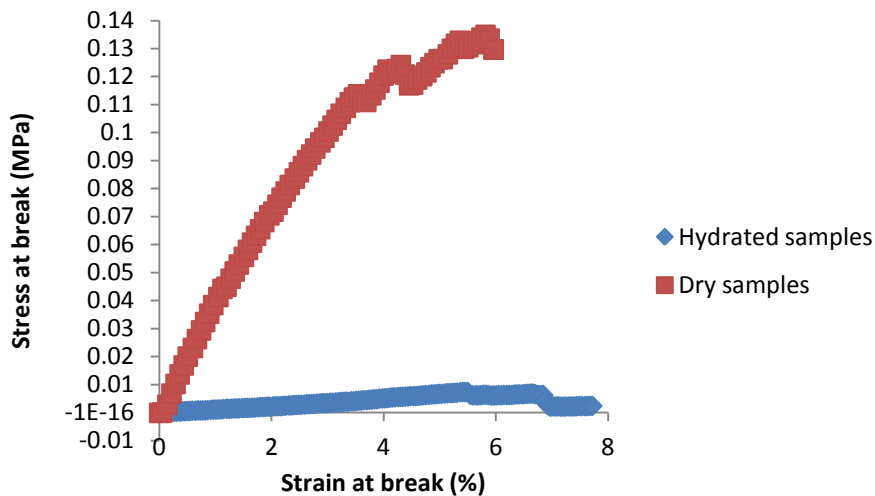


Figure 16 - Strain-stress curves of both hydrated and dry samples.

	Strain at break (%)	Ultimate Tensile Stress (MPa)	E (MPa)
Hydrated	6.64±3.49	0.02±0.02	0.19±0.05
Dry	7.09±2.58	0.18±0.08	2.91±2.20

**Table 2** - Values of strain (%), stress (MPa) and Young modulus (E) (MPa) for both hydrated and dry samples.

## 4.2.6 *In vivo* Testing

### 4.2.6.1 EPT and WRL

Table 3 (see Appendix) presents the results of motor deficit derived from EPT measures. Analyzing the results, it is possible to conclude that nerve transection (neurotmesis) caused a severe motor deficit in all experimental groups except in the Control group (Group 1). One week after the surgery, all rats in the six groups presented severe loss of hindlimb extension force except Group 1 where the sciatic nerve was un-injured. During the follow-up period of 20 weeks, it can be observed that the motor deficit of all groups decreases, with a faster recovery along time in some groups than in others. However, in the Ch-GPTMS group there is no evidence of motor deficit decrease since the results concerning this group only go as far as week 4 post-surgery. The functional analysis of this experimental group is still being performed, since the preparation and characterization of the chitosan-GPTMS guide tubes was previously needed. Two-way ANOVA revealed a significant effect of time [ $F(11,176) = 195.690$ ,  $P < 0.001$ ] and group [ $F(3,21) = 18.681$ ,  $P = 0.000$ ] in the results of motor deficit. Statistical analysis indicated that the recovery of motor function along the 20 weeks occurred faster in the End-to-end group (Group 3) followed by the Graft group (Group 4) and slower in both the PLGA group and in the Gap group (control group not included in the statistical analysis). At the end of follow-up, differences between the End-to-end group and the PLGA group (Group 5) were still significant, but no differences were observed between the PLGA group and the Graft group.

Table 4 presents the data for the WRL tests. In the first week post-surgery, all animals presented severe loss of sensory function and all tests had to be interrupted at the selected cutoff time of 12 seconds except for Group 1. Throughout the follow-up period of 20 weeks, the nociception function was being recovered and at week 20 it was in the range of normal values (below 4.3 seconds) in all the groups, except for Group 2 (Gap), which didn't present any recovery of the WRL, since the neurotmesis injury was not surgically repaired. Again, the Ch-GPTMS group has not yet reached the 20 week period but it has already shown some decrease of the WRL at week 4. Nociception recovered significantly along the following weeks [ $F(11,33) = 54.065$ ;  $P = 0.000$ ] except in the Gap group. Two way ANOVA also indicated significant differences between groups in the recovery of nociception [ $F(3,21) = 8.270$ ;  $P = 0.001$ ], with the post hoc test revealing that the End-to-end group differed from the other

three groups ( $P < 0.05$ ). At the end of 20 weeks, results of the hotplate test were similar in all four experimental treated groups. In the gap, untreated group (Group 2), no signs of recovery in sensory function were evident along 20 weeks of follow up (Table 4 - see Appendix). Values presented in Table 3 and Table 4 are plotted in Figure 17.

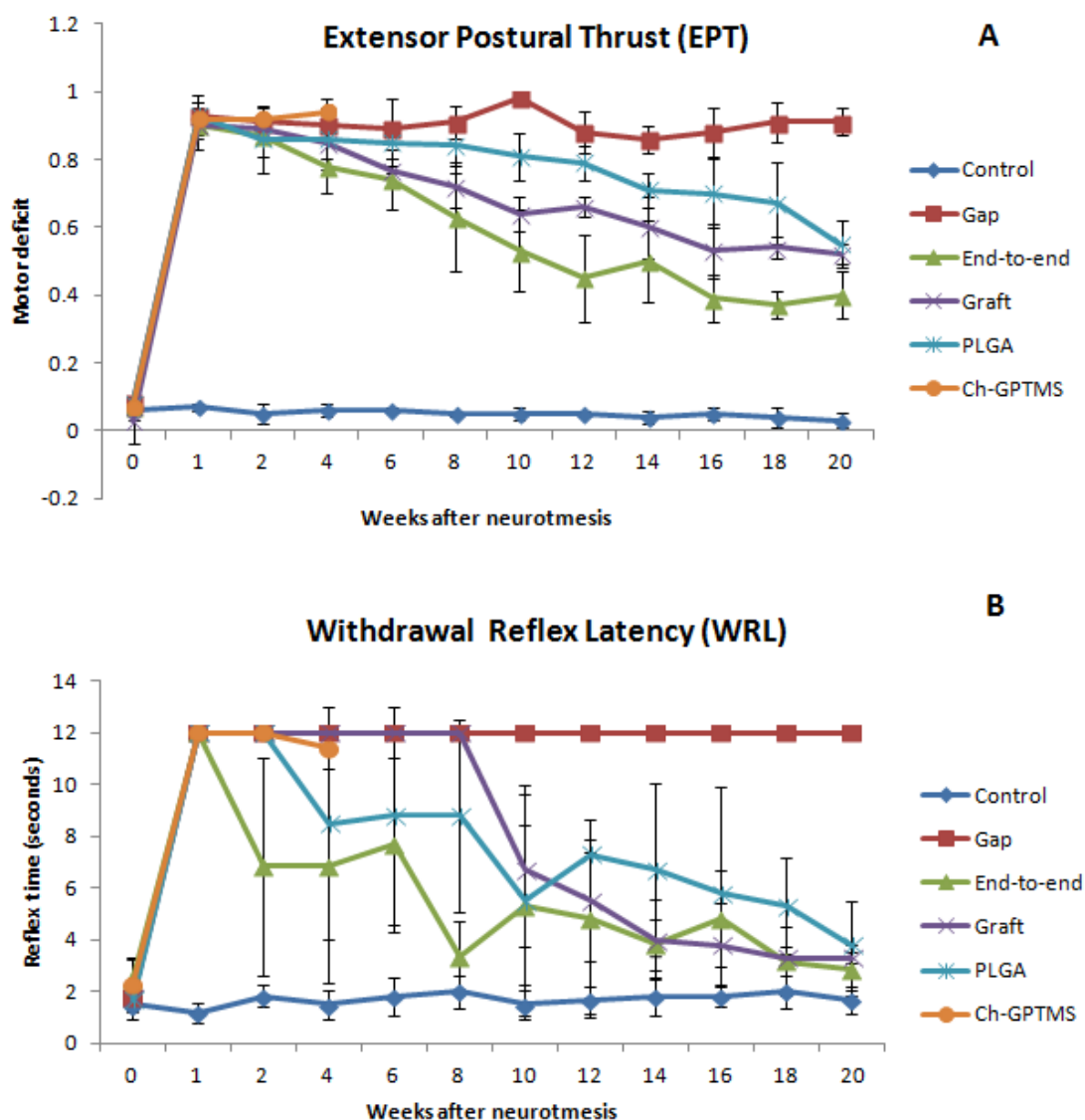


**Figure 17** - Mean Extensor Postural Thrust (EPT) and Withdrawal Reflex Latency (EPT) results for 20 weeks follow-up. Values of Motor Deficit were obtained performing EPT test (A). Values in seconds (s) were obtained performing WRL test to evaluate the nociceptive function (B). These tests have been performed pre-operatively (week 0), at week 1 and every 2 weeks after the surgical procedure until week 20, when the animals were sacrificed for morphological analysis.

#### 4.2.6.2 SFI and SSI

Both SFI and SSI were evaluated only in a small number of animals and not for all the experimental groups. At week 0 (pre-operative) SFI was  $-7.4 \pm 5.4$  in Group 2 (Gap,  $n=4$ ). One week after surgeries, SFI became much more negative and it was  $-83.2 \pm 2.2$  for group 4



(Graft, n=6). This result indicates a profound impairment in foot and toes ground contact. By the end of the follow-up period, SFI values remained highly negative which indicates only a modest recovery of the foot placement after neurotmesis. At week 20, the PLGA group (Group 5, n=5) had a SFI value of  $-62.3 \pm 2.3$  and Gap group had a SFI value of  $-82.5 \pm 4.3$ .<sup>64</sup> Variations on the SSI results were similar to SFI's. By week 20, SSI values were  $-76.6 \pm 4.9$  for Gap group.<sup>64</sup> For the Ch-GPTMS group (Group 6, n=5) SFI was  $-55.2 \pm 0.0$  in both week 1 and week 2 post-operative. At week 4, SFI became even more negative which translates the great impairment in foot and toes ground contact. As a matter of fact, it was verified in almost all experimental rats, autotomy, which limits the SFI test evaluation. On the other hand, the variations between the first two weeks after surgeries and week 4 were not as high for SSI. At week 1 and 2, SSI was  $-72.9 \pm 27.6$  and at week 4 it was  $-69.5 \pm 19.2$ . Notice that in SFI test in Group 6, it was sometimes rather difficult or even impossible to gather measurements of the impaired hindlimb since its sciatic nerve was transected which results in a highly retracted hindlimb.

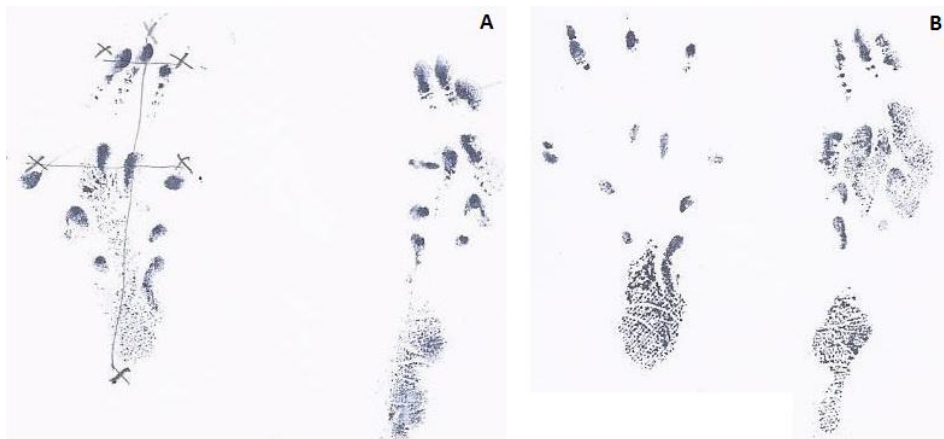


**Figure 18** - Rat footprints taken during the SSI test. On the left are represented the footprints taken on week 1 and week 2. On the right are represented the footprints taken on week 4.

#### 4.2.6.3 Stereological and histological analysis

Table 5 (see Appendix) shows the results of the stereological comparison of density, total number, mean diameter, and myelin thickness of nerve fibers in the Control, End-to-end, Graft and PLGA groups. Statistical analysis by ANOVA showed that while the intergroup numerical differences in the fiber density were not statistically significant ( $P > 0.05$ ), intergroup differences in total fiber number were not significant ( $P > 0.05$ ) between Graft and PLGA groups but was significant ( $P < 0.05$ ) in these two groups. Yet, statistical analysis of numerical data on mean nerve fiber diameter and myelin thickness revealed statistically significant ( $P < 0.05$ ) differences between all groups regarding fiber diameter, while intergroup differences in myelin thickness were not significant ( $P > 0.05$ ).<sup>64</sup>

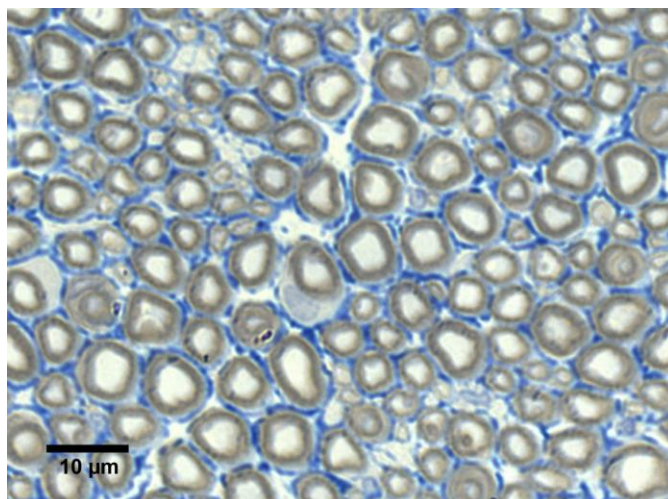


Figure 19 - Histological appearance of a normal rat sciatic nerve (Magnification: 1000x).

### 4.3 Discussion

In the present study, chitosan-GPTMS guide tubes were produced and a number of assays were performed in order to characterize them both mechanically and structurally. Furthermore, *in vivo* testing took place using the rat sciatic nerve as the experimental model. Peripheral nerve regeneration was assessed after a neurotmesis injury was induced.

The FTIR spectrum provides information through band properties, frequencies and intensities and can be used to predict chemical processes, identify species and determine the increase in the number of certain entities from the increase in the area of the band.<sup>81</sup> In Figure 12 is represented the FTIR spectrum of the chitosan-GPTMS guide tubes (A) and of the original chitosan powder (B). There are 3 peaks in the FTIR spectra of the chitosan-GPTMS guide tubes that are characteristic of the GPTMS monomer. The  $2840\text{ cm}^{-1}$  peak is assigned to the methoxy group of the GPTMS and the  $1192$  and  $914\text{ cm}^{-1}$  peaks are assigned to the epoxy group.<sup>80</sup> By introducing silane groups into chitosan through the crosslinking reaction with GPTMS, it should be visible in the FTIR spectra a peak around  $920\text{ cm}^{-1}$  that corresponds to the stretching band of Si-OH.<sup>84</sup>

The ninhydrin reaction was used to quantitatively determine the amount of free amino groups, thus calculating the degree of crosslinking of the chitosan-GPTMS guide tubes, according to a method previously described.<sup>66</sup> In this case, GPTMS, which is one of the silane-coupling agents and is constituted by an epoxy group and methoxysilane groups, is the crosslinker.<sup>8,80,85</sup> Of all the cyclic units of chitosan, 79% of them has an amino group that force-opens the epoxy group of GPTMS to form a -NH-O- bond.<sup>8</sup> During the crosslinking reaction, the epoxy group is linked to the amino group of chitosan and the methoxysilane groups are hydrolyzed forming silanol groups. These are subjected to the construction of a siloxane network due to condensation. Furthermore, the negative charges of the silanol groups and the positive charges of the amino groups favor the crosslinking reaction.<sup>8,48,80,86</sup>

Hence, the crosslinking in the chitosan-GPTMS guide tubes is achieved by two components: the epoxy and methoxysilane groups. In Figure 15 is represented the difference between the optical absorbance of the chitosan powder (non-crosslinked raw material) and the crosslinked guide tubes, being that the latter optical absorbance is rather lower than the first, which suggests that GPTMS worked as a crosslinking agent and the amount of crosslinking of the samples was 69%.

Observing Figure 11, it becomes clear that the chitosan-GPTMS guide tubes are highly porous, which in some extent is due to the presence of GPTMS that has been shown to be responsible for the size of the pores.<sup>8</sup> These chitosan-GPTMS structures were developed in order to be porous while preserving some mechanical strength. The combination of a more favorable porous microstructure and physicochemical properties, along with the presence of silicon ions may be responsible for the good results in post-traumatic nerve regeneration. Also, some degree of porosity is intended to allow for influx of low molecular nutrients required for nerve regeneration.<sup>49,87</sup> In another study, it was shown that the pore size is strongly dependent on the freezing temperature, being that the size increased with the freezing temperature.<sup>8</sup>

When developing structures of this kind, the mechanical strength is a factor to be considered in order to avoid problems during implantation and healing period such as collapsing and disintegration. The balance between hardness and flexibility should also be taken into consideration throughout their fabrication.<sup>84,88</sup> Under physiological conditions, chitosan matrices have shown to have low mechanical strength and to be unable to maintain the predefined shape after implantation.<sup>69</sup> One way to mechanically characterize the guide tubes was to plot strain-stress curves and to calculate their Young Modulus. In Figure 16 is possible to observe that the Young modulus (E), i.e. the elastic modulus, is lower for the hydrated samples, which means that when in an environment with fluids, the guide tubes are less rigid and more brittle. Thus, the guide tubes become prone to collapse than when dry.

Since chitosan-GPTMS guide tubes are highly porous, it is only logic to assume that their water uptake would be high, which is in fact demonstrated in Figure 13 that shows that after only 2 h the water uptake is 1000% of the initial dry mass of the guide tubes. It is a known fact that in the center of the bridging bond between chitosan and GPTMS there is a -Si-O-Si bond that is prone to be hydrolyzed by the NaOH solution, by which the guide tubes are washed after the first lyophilization, into S-OH bonds. Hence, it is reasonable to assume that this would allow the reduction of the tight intermolecular bonds, leave hydrophilic groups exposed and consequently allow the swelling of the guide tubes when soaked in PBS.<sup>8</sup> During the period of swelling, the porous structures are filled with PBS and sometimes go through a degradation process.<sup>8</sup> At this point, the water will occupy the atomic level space in the matrix as well as the pores. This demonstrates the ability of the matrix of the chitosan-GPTMS guide tubes to hold water, which is higher than the ability of the original chitosan.<sup>8,49,89</sup> These observations can be correlated with the SEM images of the matrix of the

guide tubes, which are very porous, thus confirming the high values of water uptake. When comparing these results with those of PLGA guide tubes, there are some differences since their water uptake occurred rapidly in the first 24 h and then stabilized until the end of the 72 h period.<sup>64</sup>

The rat sciatic nerve has been the most commonly used experimental animal model in studies concerning peripheral nerve regeneration due to its reliability.<sup>90,91</sup> Also, this experimental model provides a nerve trunk with adequate length and space at the mid-thigh for surgical manipulation and implantation of grafts or guide tubes.<sup>92</sup> Both functional and morphological assessments are evaluation tools when it is important to quantify the regeneration of the peripheral nerve considering different therapeutic strategies. Different methods should be used in order to perform an overall assessment of nerve function.<sup>87</sup> The investigation of nerve morphology can provide important information on various aspects of the regeneration process which is related to nerve function.<sup>87</sup> Chitosan-GPTMS structures have shown in *in vivo* studies an improved nerve fiber regeneration and functional recovery in neurotmesis injuries. Also, the main morphological predictors of nerve regeneration (number of fibers, axon and fiber size, and myelin thickness) were significantly improved when the rat sciatic nerve was reconstructed with such structures.<sup>27,49,50</sup>

The EPT and WRL tests have been proven to be reliable, valid and highly efficient tests when it comes to determine the functional recovery following sciatic nerve injury.<sup>93</sup> The EPT and WRL measurements also provide a quantitative measurement of motor and sensitive function recoveries, respectively, they are simple, easy to execute, and give consistently less variation between measurements.<sup>68</sup> Also, SFI tests provide a quantitative measure of degree of functional deficit, but can be cumbersome, messy, time consuming, and variable, especially considering the evaluation of neurotmesis injuries recoveries, since autotomy is frequently observed in these experimental animals. It also provides only one integrated measure of function.<sup>68</sup>

The surgical procedures allowed evaluating the performance of the chitosan-GPTMS guide tubes when in contact with fluids. The main observation was the friability of the guide tubes in a way that it was clear that the structure was fragile, which in some ways is consistent with the previously mentioned conclusions about the porosity, water uptake and mechanical strength. However, their mechanical and structural properties can be improved if a optimal ratio is achieved between chitosan and GPTMS at the time of preparation of the guide tubes.<sup>69</sup> This problem with the easiness to suture the guide tubes to the nerve stumps didn't come as problem when using PLGA guide tubes, since in this case sutures held without difficulties. However, greater care had to be taken in order to ensure the integrity of the guide tube after implantation.<sup>64</sup>

## 4.4 Conclusions

Recently, the efficacy of biomaterials and cellular systems association in the treatment of sciatic nerve axonotmesis and neurotmesis injury was tested *in vivo* using the rat model.

Animal models are used to investigate and better understand the process of a condition or a disease. An important aspect of these models is their reliability. The rat sciatic nerve has been commonly used as an experimental model in studies concerning the peripheral nerve regeneration but the functional assessment in this animal model is still a challenge.<sup>27,54</sup> The rat sciatic nerve animal model provides a not so expensive source of mammalian nervous tissue easy to manipulate and to work with. This model is used to evaluate both the motor and the sensory nerve function.<sup>54</sup> Another aspect that makes this animal model so widely used is the widespread availability and the distribution of the rat nerve trunks, which is similar to humans. Also, the induction of a crush injury in a rat sciatic nerve provides a very realistic and useful model of damage for the study of the role of numerous factors in regenerative processes.<sup>49</sup>

Following transection, axons show staggered regeneration and may take substantial time to cross the injured site and enter the distal nerve stump. However delayed axonal elongation might be caused by growth inhibition originated from the distal nerve itself, growth-stimulating influences may overcome axons stagger. As a potential source of growth promoting signals, MSCs transplantation is expected to give a positive outcome, so the future association of this cellular system to the described chitosan-GPTMS guide tubes should be tested in the near future. The guide tube was developed as a hybrid of chitosan by adding a crosslinker agent, GPTMS. A synergistic effect of an extra permeability and physicochemical properties of chitosan may be responsible for the good results in post-traumatic nerve regeneration promotion that might be observed in the sciatic nerve after neurotmesis in the end of the healing period of 20 weeks. This biomaterial may not just work as a simple mechanical device but instead may induce nerve regeneration. The neuroregenerative properties of chitosan may be explained by the effect on SCs proliferation, axon elongation and myelination.<sup>49,62,80,86</sup> Data also showed that PLC does not deleteriously interfere with the nerve regeneration process, as a matter of fact, the information on the effectiveness of PLC membranes and tube-guides for allowing nerve regeneration was already provided experimentally and with patients.<sup>87,94</sup> The MSCs isolated from the Wharton's jelly combined with PLC and chitosan-GPTMS guide tubes might be a potentially valuable tool to improve clinical outcome especially after trauma to sensory nerves, such as digital nerves.

The goals initially proposed for this experimental work were accomplished. From the mechanical and structural analysis, the chitosan-GPTMS guide tubes seem to be suitable and in some way ideal to promote the nerve regeneration after a neurotmesis injury.

## 4.5 Future Work

The process of preparation of the chitosan-GPTMS guide tubes has yet alterations and improvements to be made in order to reach optimal conditions and better results. For instance, a modification in the ratio between the amount of polymer and crosslinker can be

made during the preparation of the guide tubes. Also, a mass loss test can be performed both at physiological and acid pH in order to assess the degradation rate of the guide tubes. A sterilization method can be considered so a comparison between sterilized and non sterilized samples could be made and the differences registered. Some investigators have already sterilized chitosan-GPTMS membranes for *in vivo* testing with ethylene oxide gas but a gamma radiation sterilization can also be considered.<sup>87,94</sup> Regarding the *in vivo* tests, the follow-up of the rats implanted with the chitosan-GPTMS guide tubes will be continued until week 20. As an attempt to improve the performance of the chitosan-GPTMS guide tubes, MSCs should be combined with these structures since it has been proven to be a successful approach that led to even better results.<sup>27,62</sup>



## References

1. Gu, X., Ding, F., Yang, Y. & Liu, J. Construction of tissue engineered nerve grafts and their application in peripheral nerve regeneration. *Prog. Neurobiol.* **93**, 204-230 (2011).
2. Deumens, R. *et al.* Repairing injured peripheral nerves: Bridging the gap. *Prog. Neurobiol.* **92**, 245-276 (2010).
3. Wang, S. & Cai, L. Polymers for Fabricating Nerve Conduits. *Int. J. Polym. Sci.* **2010**, 1-20 (2010).
4. Kardas, I. *et al.* Utilization of biodegradable polymers for peripheral nerve reconstruction. *Prog. Chem. Appl. Chitin Its XV*, 159-168 (2010).
5. Radtke, C. & Vogt, P. M. Peripheral Nerve Regeneration : A Current Perspective. 434-442 (2009).
6. Gärtner, A. L. M. Association of biomaterials and mesenchymal stem cells from Wharton's jelly of human umbilical cord for promotion of peripheral nerve regeneration: A functional and morphological study. (2013).
7. Gärtner, A. *et al.* Use of poly(DL-lactide- $\epsilon$ -caprolactone) membranes and mesenchymal stem cells from the Wharton's jelly of the umbilical cord for promoting nerve regeneration in axonotmesis: in vitro and in vivo analysis. *Differentiation.* **84**, 355-65 (2012).
8. Shiroasaki, Y., Okayama, T., Tsuru, K., Hayakawa, S. & Osaka, A. Synthesis and cytocompatibility of porous chitosan-silicate hybrids for tissue engineering scaffold application. *Chem. Eng. J.* **137**, 122-128 (2008).
9. *Neuroscience.* (Sinauer Associates, 2001).
10. Armati, P. *The Biology of Schwann Cells - Development, Differentiation and Immunomodulation.* (Cambridge University Press, 2007).
11. Kuffler, S. W. & Nicholls, J. G. *The Physiology of Neuroglial Cells.*
12. Heath, C. a. & Rutkowski, G. E. The development of bioartificial nerve grafts for peripheral-nerve regeneration. *Trends Biotechnol.* **16**, 163-168 (1998).
13. Mirsky, R. & Jessen, K. R. The Neurobiology of Schwann Cells. *Brain Pathol.* **9**, 293-311 (1999).



14. Park, H.-W. *et al.* Human mesenchymal stem cell-derived Schwann cell-like cells exhibit neurotrophic effects, via distinct growth factor production, in a model of spinal cord injury. *Glia* **58**, 1118-1132 (2010).
15. Huang, Y.-C. & Huang, Y.-Y. Biomaterials and Strategies for Nerve Regeneration. *Artif. Organs* **30**, 514-522 (2006).
16. Meyer zu Hörste, G., Hu, W., Hartung, H.-P., Lehmann, H. C. & Kieseier, B. C. The immunocompetence of Schwann cells. *Muscle Nerve* **37**, 3-13 (2008).
17. Nieto, F. R. *et al.* Tetrodotoxin (TTX) as a Therapeutic Agent for Pain. *Mar. Drugs* **10**, 281-305 (2012).
18. Nectow, A. R., Marra, K. G. & Kaplan, D. L. Biomaterials for the Development of Peripheral Nerve Guidance Conduits. *Tissue Eng. Part B Rev.* **18**, 40-50 (2012).
19. Kehoe, S., Zhang, X. F. & Boyd, D. FDA approved guidance conduits and wraps for peripheral nerve injury: A review of materials and efficacy. *Injury* **43**, 553-572 (2012).
20. Gunn, S. & Cosetti, M. Processed allograft: novel use in facial nerve repair after resection of a rare racial nerve paraganglioma. *Laryngoscope* **120**, (2010).
21. Karabekmez, F. E., Duymaz, A. & Moran, S. L. Early clinical outcomes with the use of decellularized nerve allograft for repair of sensory defects within the hand. *Hand (N Y)* **4**, (2009).
22. Moore, A. M. *et al.* Acellular nerve allografts in peripheral nerve regeneration: a comparative study. *Muscle Nerve* 221-234 (2011).
23. Lundborg, G., Gelberman, R., Longo, F., Powell, H. & Varon, S. In Vivo Regeneration of Cut Nerves Encased in Silicone Tubes: Growth across a Six-millimeter Gap. *J. Neuropathol. Exp. Neurol.* 412-422 (1982).
24. Bertleff, M., Meek, M. & Nicolai, J.-P. A prospective clinical evaluation of biodegradable neurolac nerve guides for sensory nerve repair in the hand. *J. Hand Surg. Am.* **30**, (2005).
25. Whitlock, E. & Tuffaha, S. Processed allografts and type I collagen conduits for repair of peripheral nerve gaps. *Muscle Nerve* **39**, 787-799 (2009).
26. Weber, R., Breidenbach, W., Brown, R., Jabaley, M. & Mass, D. A Randomized Prospective Study of Polyglycolic Acid Conduits for Digital Nerve Reconstruction in Humans. *Plast. Reconstr. Surg.* 1036-1045 (2000).
27. Ribeiro, J. *et al.* Perspectives of employing mesenchymal stem cells from the Wharton's jelly of the umbilical cord for peripheral nerve repair. *Int. Rev. Neurobiol.* **108**, 79-120 (2013).
28. Maurício, A. C. *et al.* Cellular Systems and Biomaterials for Nerve Regeneration in Neurotmesis Injuries. 415-440 (2002).
29. Ruitter, G., Malessy, M., Yaszemski, M., Windebank, A. & Spinner, R. Designing ideal conduits for peripheral nerve repair. *Natl. Inst. Heal.* **26**, 1-15 (2010).

30. Pereira, T. *et al.* Biomaterials and stem cell therapies for injuries associated to skeletal muscular tissues. 1-26
31. Williams, D. F. The Williams Dictionary of Biomaterials. 343 (1999).
32. *Biological evaluation of medical devices – Part 6 : Tests for local effects after implantation.* (2007).
33. ISO 10993-6:2007. ISO (2007).
34. Ahmed, Z., Underwood, S. & Brown, R. A. Nerve guide material made from fibronectin: assessment of in vitro properties. *Tissue Eng.* 219-231 (2003).
35. Jiang, X., Lim, S. H., Mao, H. Q. & Chew, S. Y. Current applications and future perspectives of artificial nerve conduits. *Exp Neurol* 86-101 (2010).
36. Battiston, B., Tos, P., Cushway, T. R. & Geuna, S. Nerve repair by means of vein filled with muscle grafts I. Clinical results. *Microsurgery* 32-36 (2000).
37. Rovak, J. M. *et al.* Peripheral nerve transplantation: the role of chemical acellularization in eliminating allograft antigenicity. *J Reconstr Microsurg* 207-213 (2005).
38. Mackinnon, S. E., Doolabh, V. B., Novak, C. B. & Trulock, E. P. Clinical outcome following nerve allograft transplantation. *Plast Reconstr Surg* (2001).
39. Rivlin, M., Sheikh, E., Isaac, R. & Beredjiklian, P. K. The role of nerve allografts and conduits for nerve injuries. *Hand Clin* 435-446 (2010).
40. Grimpe, B. & Silver, J. The extracellular matrix in axon regeneration. *Prog Brain Res* 333-349 (2002).
41. Asher, R. A., Morgenstern, D. A., Moon, L. D. & Fawcett, J. W. Chondroitin sulphate proteoglycans: inhibitory components of the glial scar. *Prog Brain Res* 611-619 (2001).
42. IJkema-Paassen, J., Jansen, K., Gramsbergen, A. & Meek, M. F. Transection of peripheral nerves, bridging strategies and effect evaluation. *Biomaterials* 1583-1592 (2004).
43. Chen, P. R., Chen, M. H., Sun, J. S., Tsai, C. C. & Lin, F. H. Biocompatibility of NGF-grafted GTG membranes for peripheral nerve repair using cultured Schwann cells. *Biomaterials* 5667-5673 (2004).
44. Suzuki, K. *et al.* Histologic and electrophysiological study of nerve regeneration using a polyglycolic acid-collagen nerve conduit filled with collagen sponge in canine model. *Urology* 958-963 (2009).
45. Wu, S. *et al.* Sciatic Nerve Regeneration Through Alginate With Tubulation or Nontubulation Repair in Cat. *J. Neurotrauma* **18**, 329-338 (2004).
46. Matsuura, S., Obara, T., Tsuchiya, N., Suzuki, Y. & Habuchi, T. Cavernous nerve regeneration by biodegradable alginate gel sponge sheet placement without sutures. *Urology* (2006).

47. Hashimoto, T. *et al.* Peripheral nerve regeneration through alginate gel: analysis of early outgrowth and late increase in diameter of regenerating axons. *Exp. Brain Res.* **146**, 356-368 (2002).
48. Shiroasaki, Y. *et al.* Physical, chemical and in vitro biological profile of chitosan hybrid membrane as a function of organosiloxane concentration. *Acta Biomater.* **5**, 346-355 (2009).
49. Amado, S. *et al.* Use of hybrid chitosan membranes and N1E-115 cells for promoting nerve regeneration in an axonotmesis rat model. *Biomaterials* **29**, 4409-4419 (2008).
50. Simões, M. J., Amado, S., Gärtner, A. & Armada-da-silva, P. A. S. Use of chitosan scaffolds for repairing rat sciatic nerve defects. *Ital. J. Anat. Embryol.* **115**, 190-210 (2010).
51. Yamaguchi, I. *et al.* The chitosan prepared from crab tendon I: The characterization and the mechanical properties. *Biomaterials* **24**, 2031-2036 (2003).
52. Itoh, S., Yamaguchi, I., Shinomiya, K. & Tanaka, J. Development of the chitosan tube prepared from crab tendon for nerve regeneration. *Sci. Technol. Adv. Mater.* **4**, 261-268 (2003).
53. Evans, G. R. *et al.* Bioactive poly(L-lactic acid) conduits seeded with Schwann cells for peripheral nerve regeneration. *Biomaterials* **23**, 841-848 (2002).
54. Amado, S. Functional Assessment after Peripheral Nerve Injury - Kinematic Model of the Hindlimb of the Rat. (2012).
55. Kingham, P. J. & Terenghi, G. Bioengineered nerve regeneration and muscle reinnervation. *J. Anat.* **209**, 511-526 (2006).
56. Karaöz, E. *et al.* Human dental pulp stem cells demonstrate better neural and epithelial stem cell properties than bone marrow-derived mesenchymal stem cells. *Histochem. Cell Biol.* **136**, 455-73 (2011).
57. Lee, S.-Y. *et al.* Effects of cryopreservation of intact teeth on the isolated dental pulp stem cells. *J. Endod.* **36**, 1336-40 (2010).
58. Perry, B. C. *et al.* Collection, Cryopreservation, and Characterization of Human Dental Pulp-Derived Mesenchymal Stem Cells for Banking and Clinical Use. *Tissue Eng. Part C* **14**, 149-156 (2008).
59. Jiang, S., Liu, S. & Feng, W. PVA hydrogel properties for biomedical application. *J. Mech. Behav. Biomed. Mater.* **4**, 1228-1233 (2011).
60. Molinos, M., Carvalho, V., Silva, D. M. & Gama, F. M. Development of a hybrid Dextrin Hydrogel Encapsulating Dextrin Nanogel As Protein Delivery System. *Biomacromolecules* **13**, 517-27 (2012).
61. Molinos, M., Carvalho, V., Silva, D. M. & Gama, F. M. Development of a Hybrid Dextrin Hydrogel Encapsulating Dextrin nanogel As Protein Delivery System. *Biomacromolecules* (2012).
62. Hayakawa, S. *et al.* Use of hybrid chitosan membranes and human mesenchymal stem cells from the Wharton jelly of umbilical cord for promoting nerve regeneration in an axonotmesis rat model. *Neural Regen. Res.* **7**, 2247-2258 (2012).

63. Simões, M. J. *et al.* Use of chitosan scaffolds for repairing rat sciatic nerve defects. *Ital. J. Anat. Embryol.* **115**, 190-210 (2010).
64. Luís, A. L. *et al.* Use of PLGA 90:10 Scaffolds Enriched with In Vitro-Differentiated Neural Cells for Repairing Rat Sciatic Nerve Defects. *Tissue Eng. Part A* **14**, 979-93 (2008).
65. Luis, A. L. *et al.* PLGA 90/10 and caprolactone biodegradable nerve guides for the reconstruction of the rat sciatic nerve. *Wiley InterSci.* 125-137 (2007). doi:10.1002/micr
66. Yuan, Y. *et al.* The effect of cross-linking of chitosan microspheres with genipin on protein release. *Carbohydr. Polym.* **68**, 561-567 (2007).
67. Thalhammer, J. G., Vladimirova, M., Bershsky, B. & Strichartz, G. R. Neurologic evaluation of the rat during sciatic nerve block with lidocaine. *Anesthesiology* **82**, 1013-25 (1995).
68. Koka, R. & Hadlock, T. a. Quantification of functional recovery following rat sciatic nerve transection. *Exp. Neurol.* **168**, 192-5 (2001).
69. Maurício, A. C. *et al.* Cellular Systems and Biomaterials for Nerve Regeneration in Neurotmesis Injuries. (2011).
70. Masters, D. B. *et al.* Prolonged regional nerve blockade by controlled release of local anesthetic from a biodegradable polymer matrix. *Anesthesiology* **79**, 340-6 (1993).
71. Hu, D., Hu, R. & Berde, C. B. Neurologic evaluation of infant and adult rats before and after sciatic nerve blockade. *Anesthesiology* **86**, 957-65 (1997).
72. Luís, A. L. *et al.* Long-term functional and morphological assessment of a standardized rat sciatic nerve crush injury with a non-serrated clamp. *J. Neurosci. Methods* **163**, 92-104 (2007).
73. Bain, J. R., Mackinnon, S. E. & Hunter, D. A. Functional evaluation of complete sciatic, peroneal, and posterior tibial nerve lesions in the rat. *Plast. Reconstr. Surg.* **83**, 129-38 (1989).
74. Bervar, M. Video analysis of standing--an alternative footprint analysis to assess functional loss following injury to the rat sciatic nerve. *J. Neurosci. Methods* **102**, 109-16 (2000).
75. Dijkstra, J. R., Meek, M. F., Robinson, P. H. & Gramsbergen, A. Methods to evaluate functional nerve recovery in adult rats: walking track analysis, video analysis and the withdrawal reflex. *J. Neurosci. Methods* **96**, 89-96 (2000).
76. Raimondo, S. *et al.* Chapter 5: Methods and protocols in peripheral nerve regeneration experimental research: part II-morphological techniques. *Int. Rev. Neurobiol.* **87**, 81-103 (2009).
77. Di Scipio, F., Raimondo, S., Tos, P. & Geuna, S. A simple protocol for paraffin-embedded myelin sheath staining with osmium tetroxide for light microscope observation. *Microsc. Res. Tech.* **71**, 497-502 (2008).
78. Geuna, S., Gigo-Benato, D. & Rodrigues, A. de C. On sampling and sampling errors in histomorphometry of peripheral nerve fibers. *Microsurgery* **24**, 72-6 (2004).

79. Geuna, S., Tos, P., Battiston, B. & Guglielmo, R. Verification of the two-dimensional disector, a method for the unbiased estimation of density and number of myelinated nerve fibers in peripheral nerves. *Ann. Anat.* **182**, 23-34 (2000).
80. Shirozaki, Y. *et al.* In vitro cytocompatibility of MG63 cells on chitosan-organosiloxane hybrid membranes. *Biomaterials* **26**, 485-93 (2005).
81. Osman, Z. & Arof, a. . FTIR studies of chitosan acetate based polymer electrolytes. *Electrochim. Acta* **48**, 993-999 (2003).
82. Brugnerotto, J. *et al.* An infrared investigation in relation with chitin and chitosan characterization. *Polymer (Guildf)*. **42**, 3569-3580 (2000).
83. N, M. D., Eskandari, R., Zolfagharian, H. & Mohammad, M. Preparation and in vitro characterization of chitosan nanoparticles containing *Mesobuthus eupeus* scorpion venom as an antigen delivery system. **18**, 44-52 (2012).
84. Liu, Y.-L., Su, Y.-H. & Lai, J.-Y. In situ crosslinking of chitosan and formation of chitosan-silica hybrid membranes with using  $\gamma$ -glycidoxypropyltrimethoxysilane as a crosslinking agent. *Polymer (Guildf)*. **45**, 6831-6837 (2004).
85. Ren, L., Tsuru, K., Hayakawa, S. & Osaka, A. Novel approach to fabricate porous gelatin - siloxane hybrids for bone tissue engineering. **23**, 4765-4773 (2002).
86. Shirozaki, Y. *et al.* Challenges for Nerve Repair Using Chitosan-Siloxane Hybrid Porous Scaffolds. **2014**, (2014).
87. Ribeiro, J. *et al.* Perspectives of employing mesenchymal stem cells from the wharton's jelly of the umbilical cord for peripheral nerve repair. *Int. Rev. Neurobiol.* **108**, 79-119 (2013).
88. Harley, B. A., Hastings, A. Z., Yannas, I. V & Sannino, A. Fabricating tubular scaffolds with a radial pore size gradient by a spinning technique. *Biomaterials* **27**, 866-74 (2006).
89. Tateishi, T., Chen, G. & Ushida, T. Biodegradable porous scaffolds for tissue engineering. *J. Artif. Organs* **5**, 77-83 (2002).
90. Kerns, J. M., Braverman, B., Mathew, A., Lucchinetti, C. & Ivankovich, A. D. A comparison of cryoprobe and crush lesions in the rat sciatic nerve. *Pain* **47**, 31-9 (1991).
91. Mackinnon, S. E., Hudson, A. R. & Hunter, D. A. Histologic assessment of nerve regeneration in the rat. *Plast. Reconstr. Surg.* **75**, 384-8 (1985).
92. Van Neerven, S. G. *et al.* Retrograde tracing and toe spreading after experimental autologous nerve transplantation and crush injury of the sciatic nerve: a descriptive methodological study. *J. Brachial Plex. Peripher. Nerve Inj.* **7**, 5 (2012).
93. Gärtner, A. *et al.* Mesenchymal Stem Cells from Extra-Embryonic Tissues for Tissue Engineering - Regeneration of the Peripheral Nerve. *Adv. Biomater. Sci. Biomed. Appl.* 465-498
94. Gärtner, A. *et al.* Use of poly(DL-lactide-E-caprolactone) membranes and mesenchymal stem cells from the Wharton's jelly of the umbilical cord for promoting

nerve regeneration in axonotmesis: In vitro and in vivo analysis. *Differentiation* **84**, 355-365 (2012).

# Appendix

**Table 3 - Results of the Extensor Postural Thrust (EPT).**

Group	Week 0	Week 1	Week 2	Week 4	Week 6	Week 8	Week 10	Week 12	Week 14	Week 16	Week 18	Week 20
<b>Control</b>	0.06±0.03	0.07±0.01	0.05±0.03	0.06±0.02	0.06±0.01	0.05±0.01	0.05±0.02	0.05±0.01	0.04±0.02	0.05±0.02	0.04±0.03	0.03±0.02
<b>Gap</b>	0.08±0.01	0.93±0.04	0.91±0.01	0.90±0.02	0.89±0.09	0.91±0.05	0.98±0.02	0.88±0.06	0.86±0.04	0.88±0.07	0.91±0.06	0.91±0.04
<b>End-to-end</b>	0.07±0.01	0.90±0.07	0.87±0.06	0.78±0.08	0.74±0.09	0.63±0.16	0.53±0.12	0.45±0.13	0.50±0.12	0.39±0.07	0.37±0.04	0.40±0.07
<b>Graft</b>	0.03±0.07	0.90±0.04	0.89±0.03	0.85±0.05	0.77±0.01	0.72±0.06	0.64±0.05	0.66±0.03	0.60±0.09	0.53±0.08	0.54±0.03	0.52±0.03
<b>PLGA</b>	0.08±0.01	0.93±0.06	0.86±0.10	0.86±0.09	0.85±0.05	0.84±0.08	0.81±0.07	0.79±0.05	0.71±0.05	0.70±0.10	0.67±0.12	0.55±0.07
<b>Ch-GPTMS</b>	0.07±0.01	0.92±0.03	0.92±0.03	0.94±0.04								

Values of motor deficit, presented between 0 and 1, were obtained performing EPT test. This test has been performed preoperatively (week 0), at week 1, and every 2 weeks after the surgical procedure until week 20, when the animals were sacrificed for morphological analysis. Results are presented as mean and standard deviation (SD). In group 2 (Gap), the nerve with neurotmesis was left unrepaired. In group 3 (End-to-end), immediate coaptation with 7/0 monofilament nylon sutures of the two injured nerve endings was performed. In group 4 (Graft), the sciatic nerve was transected immediately above the terminal nerve ramification and in a 10-mm distal point. In group 5 (PLGA), the proximal and distal nerve stumps were inserted 3 mm into the PLGA guide tubes and held in place, maintaining a nerve gap of 10 mm. The nerve graft obtained, with a length of 10mm, was inverted 180° and sutured with 7/0 monofilament nylon. In group 1, the sciatic nerve was un-injured and served as control (Control). In group 6 (Ch-GPTMS, n=5), the proximal and distal nerve stumps were inserted into the guide tubes and held in place. All groups n=6.

**Table 4 - Results of the Withdrawal Reflex Latency (WRL).**

Group	Week 0	Week 1	Week 2	Week 4	Week 6	Week 8	Week 10	Week 12	Week 14	Week 16	Week 18	Week 20
Control	1.50±0.55	1.17±0.41	1.83±0.41	1.50±0.55	1.83±0.75	2.00±0.63	1.50±0.55	1.67±0.52	1.83±0.75	1.83±0.41	2.00±0.63	1.67±0.52
Gap	1.8±0.50	12±0.00	12±0.00	12±0.00	12±0.00	12±0.00	12±0.00	12±0.00	12±0.00	12±0.00	12±0.00	12±0.00
End-to-end	2.50±0.84	12.00±0.00	6.83±4.22	6.83±4.49	7.67±3.39	3.33±1.37	5.33±3.08	4.83±3.82	3.83±0.98	4.83±1.83	3.17±1.33	2.83±0.98
Graft	1.8±0.40	12±0.00	12±0.00	12±0.00	12±0.00	12±0.00	6.7±2.94	5.5±2.35	4.0±1.55	3.8±1.60	3.3±0.42	3.3±0.21
PLGA	1.7±0.52	12±0.00	12±0.00	8.5±4.46	8.8±4.22	8.8±3.71	5.5±4.46	7.3±3.08	6.7±3.33	5.8±4.12	5.3±1.86	3.8±1.72
Ch-GPTMS	2.29±0.95	12.0±0.00	12.0±0.00	11.4±0.76								

Values in seconds (s) were obtained performing WRL test to evaluate the nociceptive function. This test has been performed preoperatively (week 0), at week 1, and every 2 weeks after the surgical procedure until week 20, when the animals were sacrificed for morphological analysis. Results are presented as mean and standard deviation (SD). In group 2 (Gap), the nerve with neurotmesis was left unrepaired. In group 3 (End-to-end), immediate coaptation with 7/0 monofilament nylon sutures of the two injured nerve endings was performed. In group 4 (Graft), the sciatic nerve was transected immediately above the terminal nerve ramification and in a 10-mm distal point. In group 5 (PLGA), the proximal and distal nerve stumps were inserted 3 mm into the PLGA guide tubes and held in place, maintaining a nerve gap of 10 mm. The nerve graft obtained, with a length of 10mm, was inverted 180° and sutured with 7/0 monofilament nylon. In group 1, the sciatic nerve was un-injured and served as control (Control). In group 6 (Ch-GPTMS, n=5), the proximal and distal nerve stumps were inserted into the guide tubes and held in place. All other groups n=6.

**Table 5 - Stereological quantitative assessment of density, total number, diameter and myelin thickness of regenerated sciatic nerve fibers at week 20 after neurotmesis. Values are presented as mean ± SD.**

Group	Fiber density (N/mm <sup>2</sup> )	Fiber number (n)	Fiber diameter (µm)	Myelin thickness (µm)
Control	15.905±2.87	7,666±1.90	6.66±0.12	1.19±0.03
End-to-end	20,612±1,067	14,624±1,642	4.06±0.30	0.58±0.03
Graft	26,037±1,086	13,212±610	4.02±0.11	0.48±0.03
PLGA	21,982±1,927	10,532±2,195	3.49±0.11	0.40±0.02